12 NW

6

10.6 MICRON PARAMETRIC FREQUENCY CONVERTER

C.K. Asawa and R.L. Abrams

Hughes Research Laboratories
3011 Malibu Canyon Road
Malibu, CA 90265

December 1976

Contract N00014–75–C–0089, Mod. P00002
Final Technical Report
For Period 1 September 1974 through 31 October 1976

The views and conclusions contained in this document are those of the authors and should not be interpreted as necessarily representing the official policies, either expressed or implied, of the Advanced Research Projects Agency of the U.S. Government.

Sponsored By
DEFENSE ADVANCED RESEARCH PROJECTS AGENCY
ARPA Order No. 1806

Monitored By
OFFICE OF NAVAL RESEARCH
800 North Quincy Street
Arlington, VA 22217

ARPA Order No.	1806
Program Code Number	5E20
Effective Date of Contract	1 September 1974
Contract Expiration Date	31 October 1976
Amount of Contract	$174,956.00
Principal Investigator	R. L. Abrams (213) 456-6411, Ext. 498
Scientific Officer	Director, Physics Program Physical Sciences Division Office of Naval Research 800 North Quincy Street Arlington, Virginia 22217

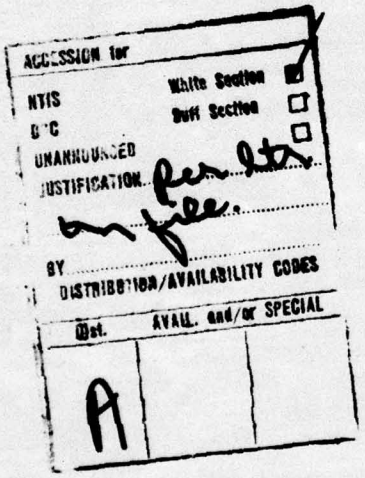

This research was supported by the Advanced Research Projects Agency of the Department of Defense and was monitored by ONR under Contract No. N00014-75-C-0089, Mod. P00002.

UNCLASSIFIED

SECURITY CLASSIFICATION OF THIS PAGE (When Data Entered)

REPORT DOCUMENTATION PAGE	READ INSTRUCTIONS BEFORE COMPLETING FORM
1. REPORT NUMBER	2. GOVT ACCESSION NO.
3. RECIPIENT'S CATALOG NUMBER: Technical	
4. TITLE (and Subtitle): 10.6 Micron Parametric Frequency Converter,	5. TYPE OF REPORT & PERIOD COVERED: Final Report, 1 Sep 74 – 30 Oct 76
	6. PERFORMING ORG. REPORT NUMBER
7. AUTHOR(s): C. K. Asawa, R. L. Abrams	8. CONTRACT OR GRANT NUMBER(s): N00014-75-C-0089, ARPA Order-1806
9. PERFORMING ORGANIZATION NAME AND ADDRESS: Hughes Research Laboratories, 3011 Malibu Canyon Road, Malibu, California 90265	10. PROGRAM ELEMENT, PROJECT, TASK AREA & WORK UNIT NUMBERS: ARPA Order No. 1806, Program Code No. 5E20
11. CONTROLLING OFFICE NAME AND ADDRESS: Defense Advanced Research Projects Agency, 1400 Wilson Boulevard, Arlington, Virginia 22209	12. REPORT DATE: Dec 76
	13. NUMBER OF PAGES: 74
14. MONITORING AGENCY NAME & ADDRESS (if different from Controlling Office): Office of Naval Research, 800 No. Quincy Street, Arlington, Virginia 22217 (12) 69 p.	15. SECURITY CLASS. (of this report): UNCLASSIFIED
	15a. DECLASSIFICATION DOWNGRADING SCHEDULE

16. DISTRIBUTION STATEMENT (of this Report)

DISTRIBUTION STATEMENT A
Approved for public release;
Distribution Unlimited

17. DISTRIBUTION STATEMENT (of the abstract entered in Block 20, if different from Report)

DDC RECEIVED JAN 31 1977 C

18. SUPPLEMENTARY NOTES

19. KEY WORDS (Continue on reverse side if necessary and identify by block number)

CO_2 laser, Nonlinear mixing, Frequency conversion, Tunable laser

20. ABSTRACT (Continue on reverse side if necessary and identify by block number)

Resonantly enhanced, single-sideband generation in a Stark tunable gas has been demonstrated, both theoretically and experimentally, for the first time. The theory was developed first; it predicted the possibility of parametric mixing of infrared and microwave radiation in deuterated ammonia ($N^{(14)}H_2D$) gas, which would result in down converted single-sideband radiation at the difference frequency. Quantitative prediction of the nonlinear effect was made and is contained in the expression for → OVER

DD FORM 1 JAN 73 1473 EDITION OF 1 NOV 65 IS OBSOLETE

UNCLASSIFIED

SECURITY CLASSIFICATION OF THIS PAGE (When Data Entered)

172 600

cont'd

the induced nonlinear coefficient. Pressure and doppler broadening effects were accounted for in the coefficient.

Successful experimental demonstration of resonantly enhanced, parametric single-sideband generation in $N^{14}H_2D$ gas was made for the first time on this contract during October 1975. The P(20) line at 10.591 μm of the $C^{12}O_2^{16}$ laser and microwave at 4.023 GHz were mixed in a microwave-optical Stark cell, yielding a newly generated downconverted wave at 10.593 μm, or 944.061 cm^{-1}. The dependences of the sideband signal on gas pressure, microwave frequency, applied dc field, and microwave power were measured and completely confirmed the theoretical predictions.

MICROMETERS

A second experiment demonstrating resonantly enhanced parametric upconversion in Stark gas was also performed. By mixing the R(18) line at 10.784 μm of the isotopic $C^{13}O_2^{16}$ laser and microwave radiation at 26.378 GHz in ammonia ($N^{14}H_3$) gas contained in a microwave optical Stark cell, upconverted parametric output at the sum frequency 928.179 cm^{-1}, or 10.774 μm, was observed for the first time. Experiments with three different microwave Stark cells of varying parametric interaction lengths with no phase mismatch are described.

PREFACE

The following personnel contributed to the research reported here. Prof. A. Yariv, a consultant to HRL, and P. Yeh of the California Insitute of Technology developed the theory of the three wave mixing in molecular Stark gas in collaboration with R. L. Abrams. The 4 and 26 GHz Stark cell development and the optical-microwave measurements were made by C.K. Asawa, T.K. Plant, A.E. Popa, and R.L. Abrams. Technical assistance was provided by R.E. Brower and R.R. Niedziejko.

MISSING PAGE
NUMBERS ARE BLANK
AND WERE NOT
FILMED

TABLE OF CONTENTS

SECTION		PAGE
	LIST OF ILLUSTRATIONS	7
I	INTRODUCTION, SUMMARY, AND CONCLUSIONS	9
	A. Introduction	9
	B. Basic Concept	9
	C. Summary of Results	11
	D. Conclusions	12
II	THEORETICAL AND EXPERIMENTAL RESULTS	15
	A. Parametric Conversion in $N^{14}H_2D$	16
	B. Parametric Conversion in $N^{14}H_3$	16
	APPENDIX A — Stark Induced Three Wave Mixing in Molecular Gases I — Theory	31
	APPENDIX B — Stark Induced Three Wave Mixing in Molecular Gases II — Experiment	45
	APPENDIX C — Broadening and Absorption Coefficients in $N^{14}H_2D$	58
	APPENDIX D — Wideband Modulation of the $C^{13}O_2^{16}$ Laser R(18) Line at 10.784 μm with an $N^{14}H_3$ Stark Cell	61

LIST OF ILLUSTRATIONS

FIGURE		PAGE
1	Simplified energy level diagram for NH_2D, showing relevant levels in an applied electric field	10
2	Low voltage $\|M\| = 6, 5, 4, \Delta M = 0$ Stark absorption spectrum of $N^{14}H_3$ with the isotopic $C^{13}O_2^{16}$ laser line R(18) at 10.874 μm	17
3	Energy levels of $N^{14}H_3$ involved in the resonant parametric interaction	19
4	TE_{10} retangular 26.378 GHz single pass cavity	23
5	SFP spectrum of the output of the single pass $N^{14}H_3$ cavity	24
6	Parametric signal versus $N^{14}H_3$ pressure for the single pass microwave cavity	25
7	Multipass and multimode cavities	27

I. INTRODUCTION AND SUMMARY

A. Introduction

We anticipate that modern optical radar systems for surveillance of orbiting objects will require new types of electro-optical devices capable of frequency control and frequency conversion of infrared (IR) laser radiation. This program addressed an approach that should lead to a new class of electro-optical devices (such as single-sideband modulators, tunable local oscillators, and frequency shifters) using the resonant interaction of optical and microwave fields in a gas whose energy level structure is controlled by an applied electric field (Stark effect).

We have demonstrated on this program, both theoretically and experimentally, that resonantly enhanced single-sideband generation can be accomplished by mixing laser and microwave radiation in a Stark-induced nonlinear gas. The initial set of experiments was performed with the $C^{12}O_2^{16}$ P(20) laser line and 4.023 GHz microwave mixed in a microwave Stark cell containing $N^{14}H_2D$. Resonantly enhanced, downconverted output as a lower sideband at 10.593 μm was generated for the first time.

A second set of experiments was performed where the R(18) line of the isotopic $C^{13}O_2^{16}$ laser and 26.38 GHz microwave radiation were mixed by $N^{14}H_3$ contained in a microwave Stark cell. Upconverted parametric output at the upper sideband at 10.774 μm was generated for the first time.

B. Basic Concept

To illustrate the basic mechanism for the interaction, consider the simplified energy level diagram of $N^{14}H_2D$ shown in Figure 1. This molecule was used in the first set of experiments. When an electric field of appropriate magnitude is applied, two $N^{14}H_2D$ energy levels (labeled 1 and 3 in Figure 1) will become resonant with the laser frequency. A third level (level 2) will also be tuned by the electric field. The key element of this system is that the applied field breaks inversion

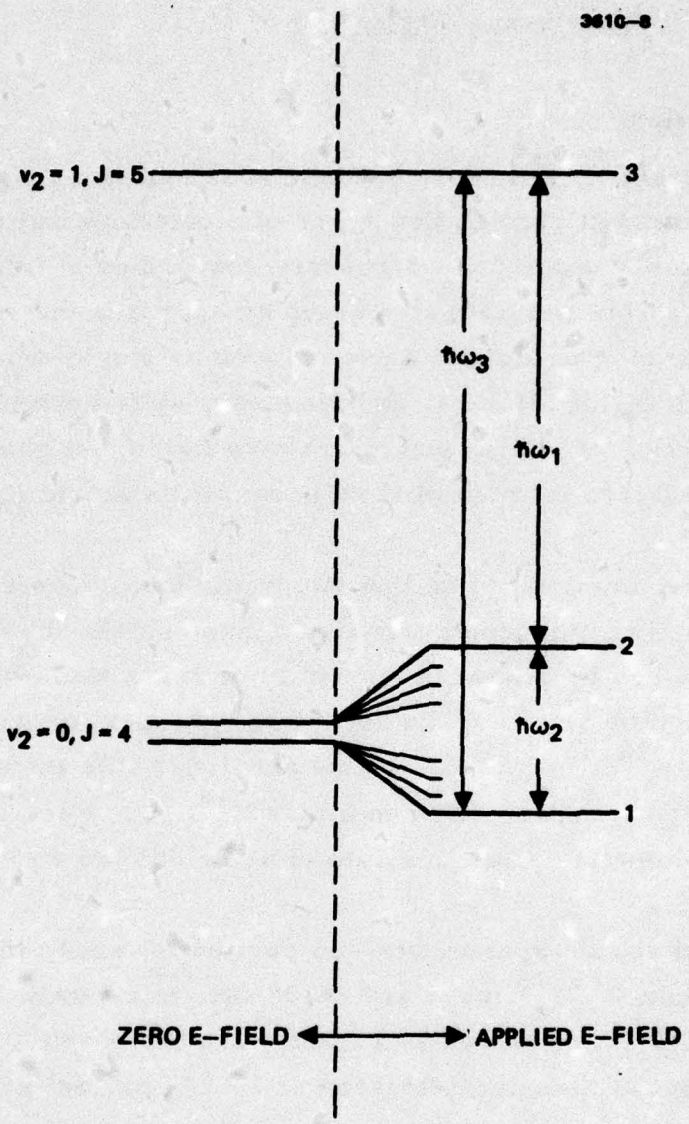

Figure 1.
Simplified energy level diagram for $N^{14}H_2D$, showing relevant levels in an applied electric field. The P(20) 10.6 μm radiation is incident at frequency ω_3, ω_2 is the applied microwave frequency, and ω_1 is the newly generated sideband frequency.

symmetry and induces a permanent dipole moment. The three electric dipole moments μ_{12}, μ_{13}, μ_{23} are all nonzero, due to the applied electric field, and this allows us to consider several possible strong interactions which would ordinarily be weak. The experiment involves simultaneously applying two fields to the $N^{14}H_2D$: an applied field at ω_2 which is resonant with levels 1 and 2 at the microwave frequency and a field at ω_3 which is resonant with levels 1 and 3 at 10.6 μm. Resonantly enhanced nonlinear mixing in the $N^{14}H_2D$ gas results in the generation of a signal at $\omega_1 = \omega_3 - \omega_2$ with measurable conversion efficiencies. A complete description is given in the Appendices. A theoretical description of this process is given in Appendix A. The first observation of parametric generation in a Stark gas is summarized in Appendix B.

In the $N^{14}H_2D$ system, the parametric output at ω_1 is downconverted where ω_1 $(= \omega_3 - \omega_2)$ is resonant with levels 2 and 3. In contrast, the parametric output ω_1 for $N^{14}H_3$ (described in Section II-B) is upconverted where ω_1 $(= \omega_3 + \omega_2)$ is resonant with levels 1 and 3. ω_3 is resonant with levels 2 and 3, not with levels 1 and 3 as in $N^{14}H_2D$.

C. Summary of Results

The theory of resonantly enhanced three wave mixing in a Stark molecular gas was developed first. It predicted the experimental possibility of the mixing. We have shown how the application of a dc Stark field destroys the basic inversion symmetry of a Stark molecular gas and allows resonantly enhanced parametric mixing to occur. We have derived an expression for the nonlinear coefficient which describes the mixing of an infrared and microwave field in $N^{14}H_2D$ and the generation of a new downconverted infrared field. The effect of pressure and doppler broadening of the resonant transitions has been considered in the expression for the coefficient.

The first observation of resonantly enhanced, dc induced, three wave mixing in a Stark gas was made under this contract. The P(20) line at 10.591 μm (944.195 cm^{-1}) of the $C^{12}O_2^{16}$ laser and microwave at 4.023 GHz (0.134 cm^{-1}) were mixed in a deuterated ammonia cell, resulting in the generation of infrared at 10.593 μm (944.061 cm^{-1}).

The parametric output was downconverted at the difference frequency of the laser line and the microwave. The dependence of the generated signal on gas pressure, microwave frequency, applied dc field, and microwave power were determined; the results precisely confirmed the theoretical predictions. The maximum conversion efficiency for the parameters used was expected to be 0.27%, a value close to the observed value of 0.2%.

Parametric upconversion in a Stark gas was also observed for the first time on this program. The R(18) line at 10.784 μm (927.300 cm^{-1}) of the isotopic $C^{13}O_2^{16}$ laser and microwave at 26.378 GHz (0.879 cm^{-1}) was mixed in ammonia ($N^{14}H_3$) gas contained in a microwave-optical Stark cell, resulting in an upconverted single-sideband output at the sum frequency of 928.179 cm^{-1}, or 10.774 cm^{-1}. The theoretical nonlinear coefficient for the $N^{14}H_3$ system was 1.01×10^{-20} f/v (MKS units), more than 40 times greater than that of the initial $N^{14}H_2D$ system. With low microwave power of 95 mW, the experimentally observed conversion efficiency was 0.15% for the 2.2 cm cavity, close to the theoretically calculated value of 0.11%. With greater microwave power (1 W) and an interaction length of 9 cm, conversion efficiencies of 3% are attainable.

D. Conclusion

It was demonstrated theoretically and experimentally on this program that mixing infrared laser radiation and microwave radiation in a Stark molecular gas results in the generation of new infrared radiation at the sum or difference frequencies of the input radiation. These new single-sidebands expand the coverage of the infrared region.

By modulating the microwave (AM, FM, or pulsed), these newly generated sidebands will themselves be modulated. We anticipate that future optical radar surveillance systems will find such a modulation format and related electro-optical microwave devices useful.

To expand the use of this technique to generating new single-sidebands will require making an experimental survey of Stark resonances of all known polar molecules with all the strong infrared laser lines. Those resonances with molecules having optimum Stark mixing of levels and strong optical and microwave absorptions should lead to useful parametric converters.

II. THEORETICAL AND EXPERIMENTAL RESULTS

Resonantly enhanced, dc induced, three wave mixing in Stark gases was investigated under this contract. The purpose was to generate new radiation frequencies at either the sum (upconverted) or difference (downconverted) frequencies of two input waves.

Three wave mixing in a gas is possible when an external perturbation destroys the normal macroscopic inversion symmetry of the gas. This condition occurs when an electric Stark field is applied to a polar molecular gas. The mixing interaction with such a gas will be small (with low field intensities of the waves) due to the low densities of the gas. Mixing interaction can be greatly increased by resonant enhancement, that is, by selecting appropriate Stark molecular gases with energy level transitions which are resonant with all three waves.

We have investigated in detail two such gaseous systems and their parametric interactions. First, the $N^{14}H_2D$ (deuterated ammonia) gas, which mixes the P(20) line at 10.591 μm (944.195 cm^{-1}) of the $C^{12}O_2^{16}$ laser and 4.023 GHz (0.134 cm^{-1}) microwave, resulting in a downconverted single sideband parametric output at the difference frequency 944.061 cm^{-1}, or 10.593 μm wavelength. Second, the $N^{14}H_3$ (ammonia) gas, which mixes the R(18) line at 10.784 μm (927.300 cm^{-1}) of the isotopic $C^{13}O_2^{16}$ laser and 26.378 GHz (0.879 cm^{-1}) microwave, resulting in an upconverted single-sideband parametric output at the sum frequency 928.179 cm^{-1}, or 10.774 μm.

The theory of the resonantly enhanced mixing in the Stark gas was first investigated under this contract. The effect of doppler and pressure broadening on the induced nonlinear coefficient was calculated. The theory was then applied to the $N^{14}H_2D$ system. Subsequent experiments with $N^{14}H_2D$ completely confirmed the theoretical results.

The theoretical and experimental investigation of the second system, $N^{14}H_3$ with the R(18) line of the $C^{13}O_2^{16}$ laser and 26.386 GHz microwave, is presented in some detail in Section II-B. Properties of $N^{14}H_3$, such as its (exceptionally high) absorption coefficient, energy levels, and the first observation of the upconverted signal with this molecule and other details are presented there.

A. Parametric Conversion in $N^{14}H_2D$

The first observation of resonantly enhanced, dc induced, three wave mixing in a gas ($N^{14}H_2D$) was made under this contract during October 1975, well after the quantitative theory of the interaction had been developed. The theory of the interaction for the $N^{14}H_2D$ molecule and the predicted value of the nonlinear coefficient are given in Appendix A. The experimental observations are given and analyzed in Appendix B. Related pressure broadening measurements of $N^{14}H_2D$ absorption lines are given in Appendix C. These results were described in previous contract reports.

B. Parametric Conversion in $N^{14}H_3$

High parametric gain potential is promised by the $N^{14}H_3$ (ammonia) molecule, using the R(18) line of the isotopic $C^{13}O_2^{16}$ laser. The very strong resonance between the R(18) line and $N^{14}H_3$ absorption line was discovered at HRL during experiments to determine new resonances for laser stabilization and laser amplitude modulation applications (Appendix D). The $N^{14}H_3$-$C^{13}O_2^{16}$ system was later examined as a potential parametric converter. (Such a converter would have practical advantages in that the isotopic $C^{13}O_2^{16}$ lines are less absorbed by normal atmospheric constituents than lines of the common $C^{12}O_2^{16}$ laser.) The small amount of mixing of the ground states of $N^{14}H_3$ by the Stark fields, due to the large inversion splitting in the ground states, initially suggested that this system had poor potential as a parametric mixer. (Mixing permits the optical transition at the parametric frequency.) However, detailed examination indicated that more than an order of magnitude greater gain over the $N^{14}H_2D$ can be obtained with the new system, due to the very strong optical transitions between the rotational-vibrational levels overcoming the weak mixing of the ground states.

Figure 2 shows the Stark absorption spectra of the $|M| = 6$, 5, and 4, $\Delta M = 0$ transitions. The peak absorption occurred with 1000, 1200, and 1500 V over a gap of 0.153 cm. With an $N^{14}H_3$ pressure of 0.47 Torr and a Stark voltage of 1000 V, nearly complete absorption

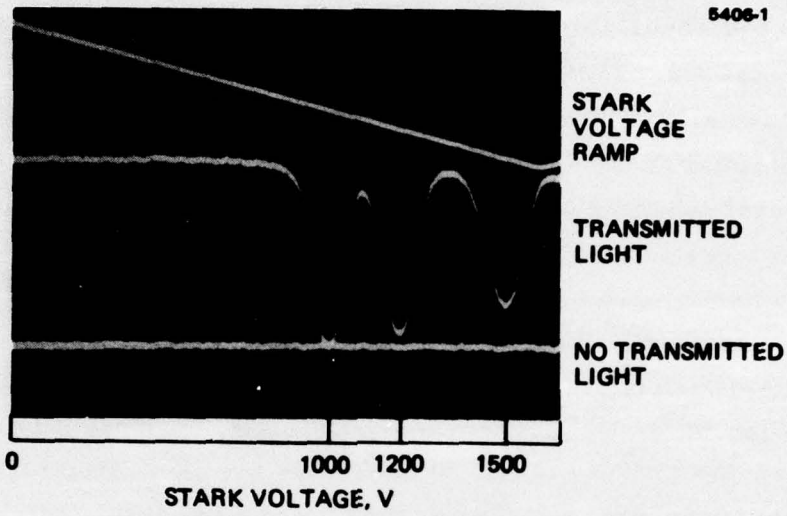

Figure 2.
Low voltage $|M| = 6, 5, 4, \Delta M = 0$ Stark absorption spectrum of $N^{14}H_3$ with the isotopic $C^{13}O_2^{16}$ laser line R(18) at 10.784 μm. Pressure, 0.47 Torr; path length, 10 cm; Stark gap, 0.153 cm. Upper trace is the Stark voltage ramp. The "no transmitted light" trace was triggered separately.

of the R(18) laser line over a 10 cm path length was observed. The low-pressure absorption coefficient was measured at 0.2 to 0.3 Torr to be 0.85 ± 0.15 cm^{-1} Torr^{-1}, about 40 times that of $N^{14}H_2D$.

The energy levels of $N^{14}H_3$ involved in the transitions corresponding to the absorption lines of Figure 2 are shown in Figure 3. The transitions were identified on the basis of the precision $C^{13}O_2^{16}$ laser line tabulations by Freed et al.[1] and the spectroscopic study of $N^{14}H_3$ by Shimizu.[2]

Several features distinguish the $N^{14}H_3$ from the $N^{14}H_2D$ parametric mixer system. First, the R(18) laser resonance takes place between the upper "ground" state and a higher state, with the parametric resonance taking place between the latter state and the lower "ground" state. Upconversion occurs for $N^{14}H_3$ in contrast to downconversion for $N^{14}H_2D$. Second, there is relatively little mixing of the "ground" $|a\rangle$ and $|s\rangle$ states of $N^{14}H_3$ by the Stark field; this results in small transition probabilities at the parametric frequency. The relatively small quadratic Stark splitting, and therefore the small amount of mixing, arises from the large zero field inversion splitting of 25 GHz. In $N^{14}H_2D$ the zero field ground splitting is small and is due to near accidental degeneracy of inversion split adjacent $J_{K_{-1}K_1}$ levels. This results in a large Stark effect and therefore a high degree of mixing of states. Third, the $|a\rangle$ to $|s\rangle$ electric dipole optical transitions of $N^{14}H_3$ involved in the parametric process are several times greater than the $|a\rangle$ to $|a\rangle$ optical transitions involved in $N^{14}H_2D$. The net result is that the high transition probability in $N^{14}H_3$ overcomes the small mixing of the "ground" state levels such that the ammonia system promises more than an order of magnitude greater parametric gain than the $N^{14}H_2D$ system for equal microwave powers.

---

[1] C. Freed, A.H.M. Ross, and R.G. O'Donnell, J. Mol. Spectrosc. 49, 439 (1974).

[2] F. Shimizu, J. Chem. Phys. 52, 3572 (1970).

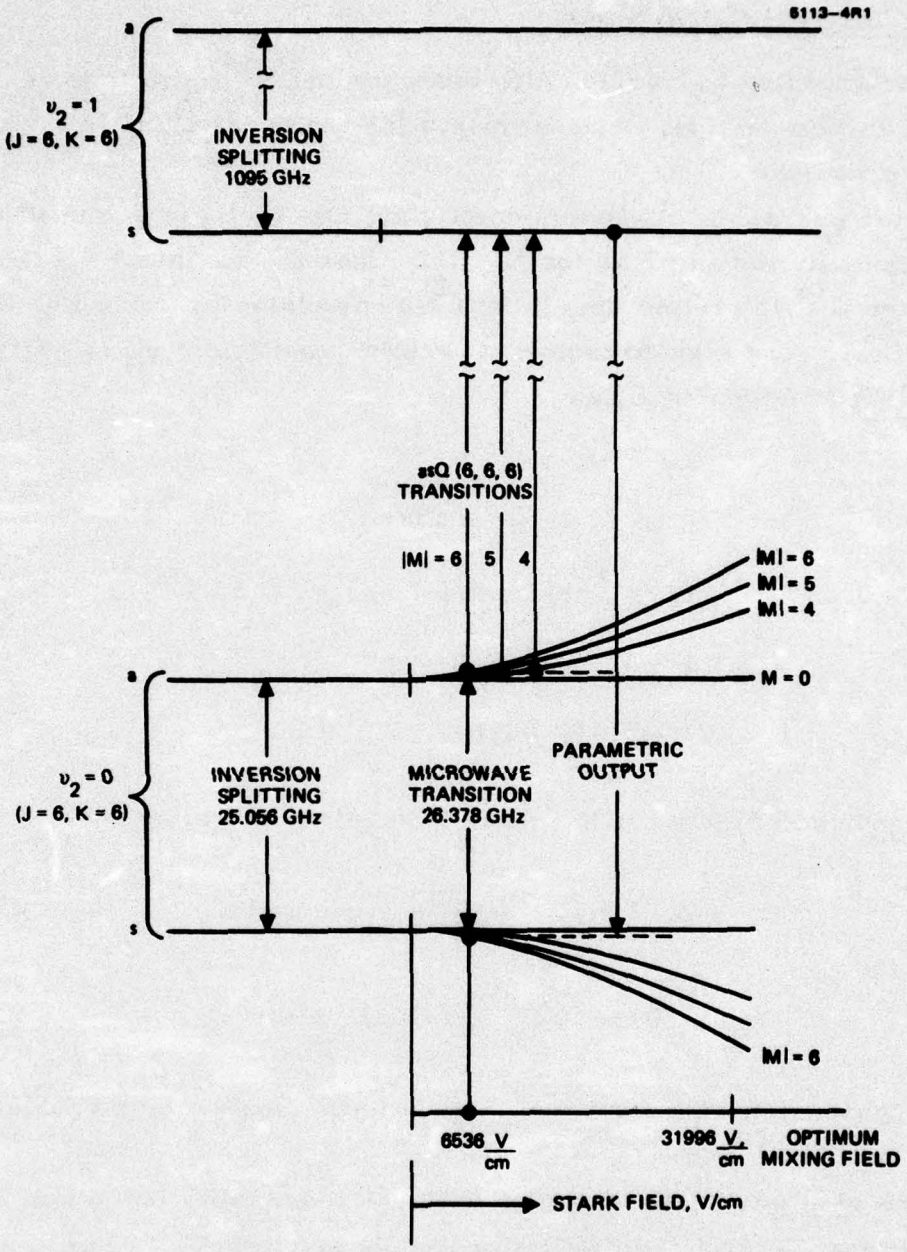

Figure 3.
Energy levels of $N^{14}H_3$ involved in the resonant parametric interaction. The $C^{13}O_2^{16}$ R(18) laser line is resonant with the asQ(6,6,6) transition. The parametric output is up-converted. The s → s transition is forbidden in this symmetric top with zero Stark field. The $|M| = 6, 5, 4$, $\Delta M = 0$ transitions are indicated, corresponding to the absorption lines of Figure 1.

1. Theoretical Calculations

The expected conversion efficiency for the $N^{14}H_3$ system is calculated in this section. Requirements for phase matching in a waveguide are presented.

If the pressure broadening coefficient for $N^{14}H_3$ is assumed to be approximately the same as for $N^{14}H_2D$, then the nonlinear coefficient for the $N^{14}H_3$ system may be readily calculated by using Eq. (8) of Appendix A. The high-pressure absorption coefficient γ_H is written, using Eq. (7) of Appendix A, as

$$\gamma_H = \frac{\alpha_3}{\sqrt{\pi} \times F(x)} \quad , \tag{1}$$

where $\alpha_3 = 0.85\ \text{cm}^{-1}\ \text{Torr}^{-1}$ times the pressure P of $N^{14}H_3$

$$x = c\Gamma/\sqrt{2}\,\sigma\,\omega_{32}$$

$$\Gamma = 2\pi\,(20.1)P\ \text{MHz} \quad .$$

The nonlinear coefficient for $N^{14}H_3$ is then calculated to be

$$d = 2.73 \times 10^{-6}\ \frac{\text{cm}}{\text{stat V}}\ \text{(esu units)} \tag{2}$$

$$d = 1.01 \times 10^{-20}\ \frac{F}{V}\ \text{(MKS units)} \quad . \tag{3}$$

The nonlinear coefficient for $N^{14}H_3$ is more than forty times greater than that for the $N^{14}H_2D$ system.

The gain g is proportional to the nonlinear coefficient d and to the microwave electric field intensity E_2, as given in Eq. (1) of Appendix B. For the experiments with $N^{14}H_3$, the microwave power was limited by the maximum output of the klystron at 26 GHz of 0.095 W. With this limitation, the gain is calculated to be $g = 0.044\ \text{cm}^{-1}$ for 0.9 Torr of $N^{14}H_3$.

With 1 W of microwave power, the gain g is 0.143 cm^{-1}; with 4 W input, g = 0.286 cm^{-1}. The latter value is more than ten times greater than that for the $N^{14}H_2D$ system with 4 W input at 4 GHz. However, with 4 W of 26 GHz microwave power, microwave power saturation effects are expected to affect the parametric processes.

Phase mismatch affects the parametric processes. In a three wave interaction where one of the waves is microwave spatially constrained to the waveguide, phase mismatch will occur if the optical waves propagate along the waveguide axis. By propagating the optical waves at an angle θ with respect to the axis, however, the phase mismatch may be reduced to zero. The angle is determined for a rectangular waveguide of width a as $\theta = \tan^{-1}(k_c/k_g)$, where $k_c = \pi/a$ is the cutoff wave vector and $k_g = \sqrt{3}(\pi/a)$ is the guide wave vector when the microwave free space wavelength λ_2 is equal to a. Phase mismatch is zero ($\Delta k = 0$) when the optical waves propagate at an angle $\theta = 30°$ with the waveguide axis and in the plane of the broad side of the waveguide. Note that, if the optical waves were propagated along the waveguide axis for $\lambda_2 = a = 1.14$ cm, Δk would be very large: $\Delta k = 0.74\ cm^{-1}$.

When $\Delta k = 0$, the expression for the conversion efficiency (Eq. (2) of Appendix B) is simplified to

$$\eta = \frac{g^2 \exp\left(\frac{-\alpha_3 x}{2}\right)}{\left[\frac{\alpha_3^2}{4} - g^2\right]} \sinh^2\left\{\left[\frac{\alpha_3^2}{4} - g^2\right]^{1/2} \frac{x}{2}\right\}, \quad \text{for } g^2 < \tfrac{2}{3}/4 , \tag{4}$$

where $\alpha_3 = 0.85 \times P\ cm^{-1}$, P = pressure in Torr, and α_1 (= 0.02 α_3 for the NH_3 system) has been neglected. For $g^2 < \alpha_3^2/4$, g^2 and $\alpha_3^2/4$ are interchanged and $\sinh^2$ changed to $\sin^2$.

The optimum interaction distance is given by

$$(x)_{opt} = \frac{2}{\left[\frac{\alpha_3^2}{4} - g^2\right]^{1/2}} \tanh^{-1}\left\{\frac{2}{\alpha_3}\left[\frac{\alpha_3^2}{4} - g^2\right]^{1/2}\right\} . \tag{5}$$

For $g^2 > \alpha_3^2/4$, g^2 and $\alpha_3^2/4$ are interchanged and $\tanh^{-1}$ replaced by $\tan^{-1}$.

For $N^{14}H_3$ at P = 0.9 Torr, we have g = 0.044 cm^{-1} and $\alpha_3 = 0.85 \times 0.9$ cm^{-1}. The optimum interaction distance is then $(x)_{opt}$ = 15.1 cm for the pressure P = 0.9 Torr. The conversion efficiency for the 15.1 cm interaction distance is $(\eta)_{opt} = 0.0032$, or 0.32%. For a 2.2 cm path length, the conversion efficiency is calculated to be 0.11%. This illustrates that for a gain 0.044 cm^{-1}, the maxima is very broad.

With 1 W of microwave power, g = 0.143 cm^{-1}, $(x)_{opt}$ = 9.24 cm, and $(\eta)_{opt}$ = 2.9%. Note that in these calculations the microwave field and therefore the gain are kept constant; if the cavity size is increased, the field and therefore the gain will be reduced for the same microwave input power.

2. Experimental Results

A TE_{10} rectangular cavity was constructed for 26 GHz (Figure 4). For phase matching, the optical beam was propagated at 30° to the cell axis in the plane of the broad face of the cavity. A vacuum-tight, tunable short on one side of the cavity permitted continuous selection of cavity resonances. The microwave was hole-coupled to the cavity and the hole was vacuum sealed with a thin wafer of mica. Careful selection of hole size and mica thickness resulted in critical, or "matched," coupling. The maximum output of the microwave source (OKI klystron 24V11) at 26.5 GHz was 0.095 W.

The optical and electronic system to detect the parametric output was described in Appendix B. A SFP trace showing the upconverted parametric output at 10.774 μm is given in Figure 5. The laser beam passed through the $N^{14}H_3$ gas also appear on the SFP trace.

The parametric output versus $N^{14}H_3$ pressure for the single-pass cavity was measured and is shown in Figure 6. Unfortunately, pressures higher than 0.9 Torr resulted in Stark field breakdown of the $N^{14}H_3$ gas. The curve shows the slow rise of the parametric output at low pressure, as predicted by theory. The approach towards saturation at higher pressures is obscured by the optical absorption of the

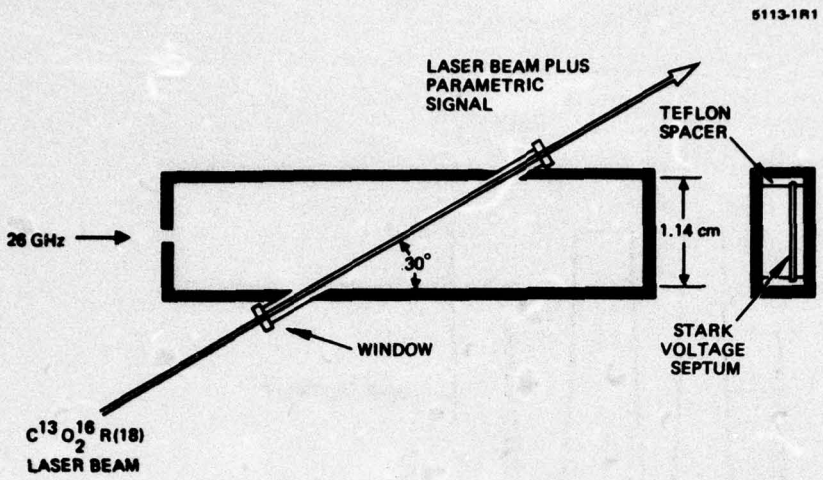

a

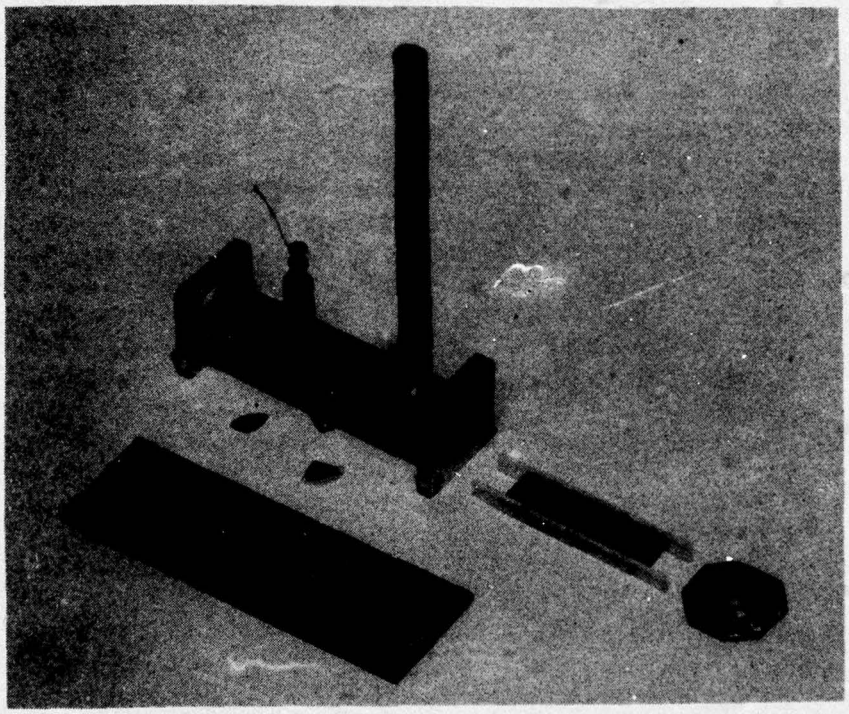

b

Figure 4.
TE_{10} rectangular 26.378 GHz single pass cavity. (a) Schematic illustrates optical beams propagating at 30° to cell axis in order to phase match with the waveguide mode of the microwave radiation. The optical wave passed through the narrower gap between the system and the waveguide. (b) Photograph of the cavity. A tuning short permitted precise tuning of the cavity. 95 mW of microwave power was critically "hole" coupled to the cavity.

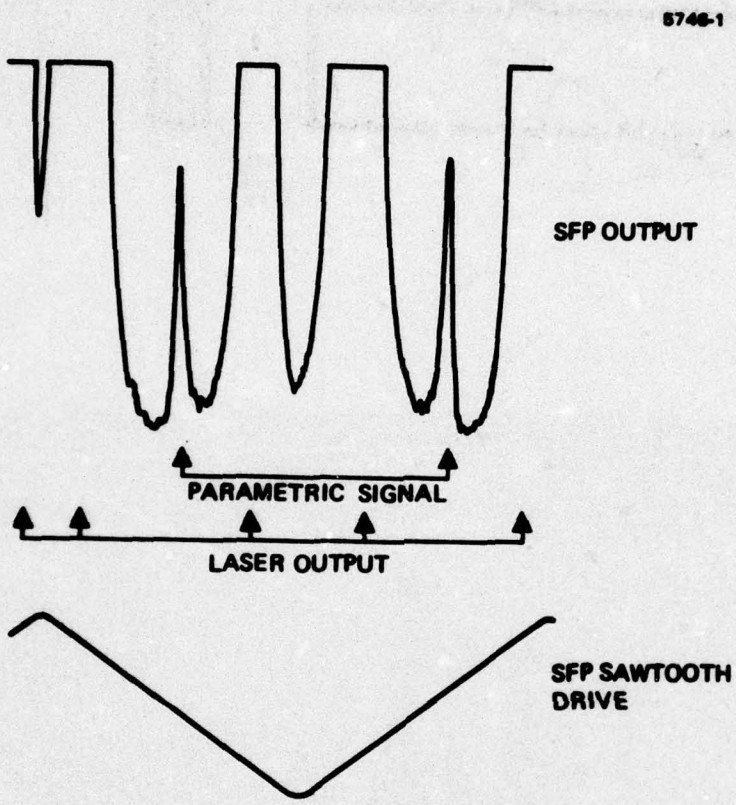

Figure 5.
SFP spectrum of the output of the single pass $N^{14}H_3$ cavity. The parametric signal and the laser beam transmitted through the cell appear in the output. SFP mirror spacing = 1.39 cm.

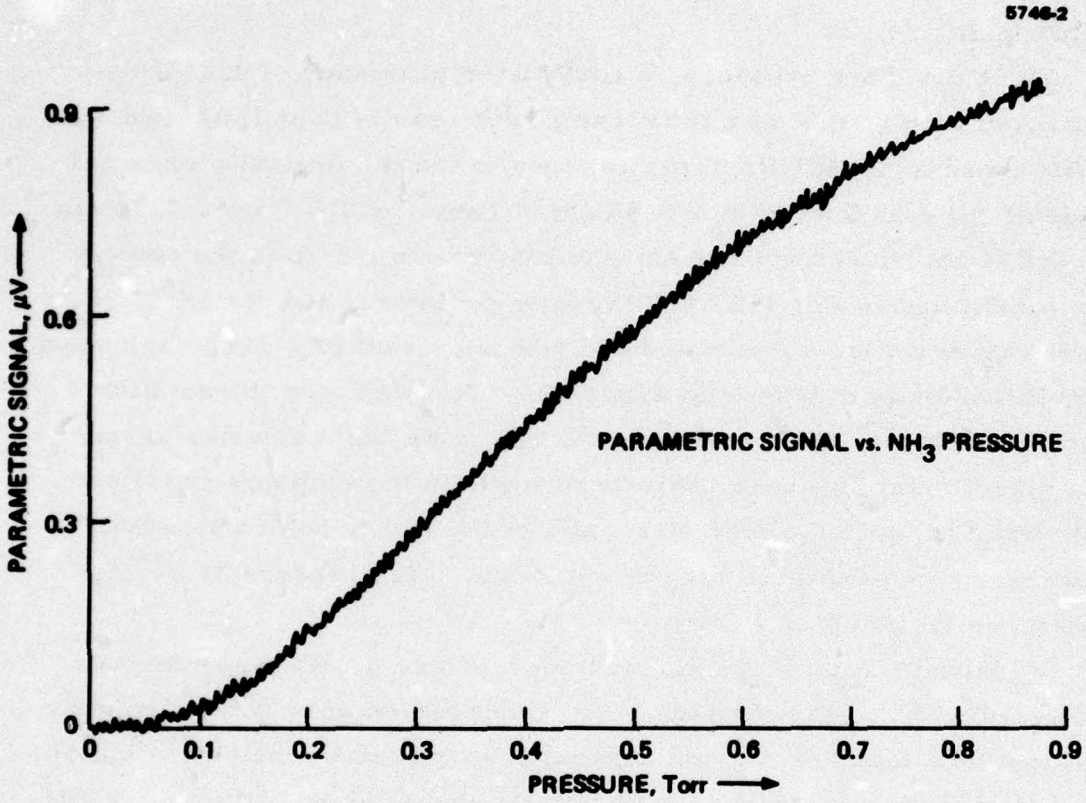

Figure 6. Parametric signal (detector output) versus $N^{14}H_3$ pressure for the single pass microwave cavity. Electrical breakdown occurred intermittently between 0.7 and 0.9 Torr. The curve indicates saturation at higher pressures due to pressure broadening; the curve is also dependent upon the absorption of the optical waves.

parametric signal at the higher pressures of Figure 6. For example, at 0.9 Torr, the parametric power level is attenuated by a factor of 0.43 in the 2.2 cm cell. The attenuation results from the exponential factor in Eq. (4).

At 0.9 Torr pressure, a conversion efficiency of 0.15% was measured with 95 mW of microwave power, cavity Q of 1500, and the cavity tuned to 26.38 GHz. This is close to the theoretically expected value of $\eta = 0.11\%$ when $\alpha_3 = 0.85\ \text{cm}^{-1}\ \text{Torr}^{-1} \times 0.9\ \text{Torr} = 0.76\ \text{cm}^{-1}$, $g = 0.044\ \text{cm}^{-1}$, and $x = 2.2$ cm (the interaction length in the cavity) are substituted in Eq. (4). To increase the interaction distance, two other cavities were constructed and tested: a multiple-pass cavity and a multimode cavity (shown in Figure 7). To extend the interaction distance to 11 cm, four reflections off the side walls and five passes in a direction at 30° to the axis were made in the multipass cavity. Gold was evaporated on the side walls of the cavity before assembly. However, no measurable parametric output was observed at $N^{14}H_3$ pressures from 0 to 0.7 Torr.

Subsequent analysis pointed out a problem with the multipass cavity. Due to π phase change by all three waves upon reflection, the parametric buildup during one traversal is undone by the reflection of the wall and the second traversal through the medium. The net result is residual output, primarily due to the last traverse if there is an odd number of traverses and if absorption is not complete. The analysis follows. Consider one of the equations of B(1) in Appendix B where the absorption is neglected. The parametric buildup dA_1 takes place along x during the first traversal (see Figure 7(a)) as

$$\frac{dA_1}{dx} = \xi A_2 A_3 \ . \qquad (6)$$

After reflection, the A_1, A_2, and A_3 phases are changed by π. However, according to the above equation, the phase of dA_1 is not changed. Thus, during the second traversal through the cavity, the amplitude A_1 is severely attenuated. If amplitudes A_2 and A_3 remain constant, A_1 would be zero at the end of the second traversal.

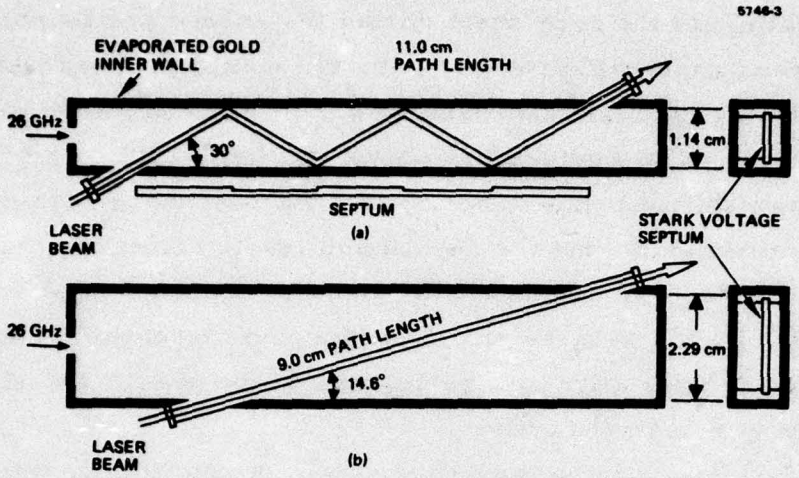

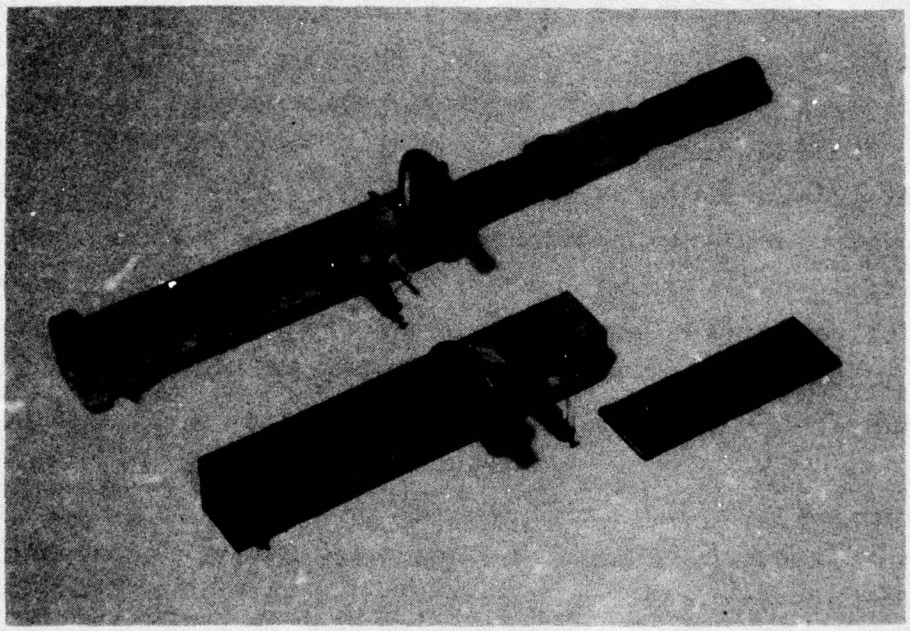

c

Figure 7.
Two other cavities constructed (a) multipass TE_{10} cavity, 13.5 cm length 1.14 cm width. (b) Multimode cavity 13.2 cm length, 2.29 cm width. (c) Photograph of the two cavities.

To eliminate the decrement during the second and fourth traversal in the multipass cavity (Figure 7(a)), the resonance process was eliminated by reducing the Stark field during the second and fourth pass. To do this, the septum was notched as shown in Figure 7(a). The Stark absorption was shifted to the wings so that the resonance parametric process was inactive during the second and fourth traverses. Conversion during the first, third, and fifth pass was expected to be cumulative. However, even with the modifications, no measurable output was observed. No further work was performed on the multipass cell in favor of a study of a final cavity.

The last cavity to be investigated was the multimode microwave cavity shown in Figure 7(b). To increase the interaction distance to 9 cm, the cavity was widened to decrease the cutoff frequency of the fundamental mode. Three cavity modes were possible, the TE_{10}, TE_{20}, and TE_{30} modes. Optical mixing with only the fundamental TE_{10} mode was desired. The TE_{10} mode waveguides are at the angle of 14.6° to the axis in the plane of the broad face of the cavity. The cavity was again critically hole-coupled to the microwave source. At a pressure of 0.47 Torr, septum to ground discharge occurred, limiting the maximum pressure to this value; conversion efficiency of 0.05% was measured. Extrapolating to 0.9 Torr, conversion efficiency is 0.10%. The theoretical efficiency is 0.2% at 0.9 Torr and a 9 cm interaction distance.

With the above multimode and multipass cavities, the cavity Q's are reduced by a factor of about three or more over that of the single-pass cavity. In these cavities, the cavity volumes are considerably larger, thereby decreasing the effective microwave fields. The resulting loss in microwave electric field decreases the conversion efficiency.

To summarize this section, the experimentally observed conversion efficiencies with the $N^{14}H_3$ system for the short single-pass cavity and the multimode cavity have confirmed the theoretical calculations. The experimentally observed conversion efficiencies were about 0.1% with the low microwave power used. No output was observed with the multiple reflection (multipass) cavity; the source of the problem is not known.

With 1 W of microwave power input and by optimizing the interaction distance to 9 cm, nearly 3% conversion efficiency is possible with a cavity similar to the single-pass cavity. However, the interaction distance must be increased without increasing the cavity volume (to keep the microwave field constant). This will require the innovation of a new multipass structure that solves the reflection problem noted above.

APPENDIX A

Stark Induced Three-Wave Mixing in Molecular Gases[†]

I. Theory

R. L. Abrams

Hughes Research Laboratories, Malibu, CA 90265

A. Yariv and P. Yeh[††]

California Institute of Technology, Pasadena, CA 91109

ABSTRACT

Application of a dc electric field to a gaseous system destroys the basic inversion symmetry and allows three-wave mixing processes to occur. A theoretical derivation of this effect under conditions of resonantly enhanced nonlinearities is given for a three-level system. Calculations are presented for mixing of a CO_2 laser with 4 GHz microwaves in the molecule NH_2D, producing single lower sideband radiation.

[†] Supported in part by the Advanced Research Projects Agency, monitored by the Office of Naval Research

[††] Supported by the Army Research Office, Durham, N.C.

I. INTRODUCTION

Nonlinear optical mixing in atomic vapors has been demonstrated for a number of different processes including third harmonic generation,[1-4] dc induced second harmonic generation,[5,6] infrared upconversion,[7,8] and multiphoton generation of new wavelengths.[9] Resonant enhancement and phase matching of three-photon processes has led to rather impressive conversion efficiencies for certain interactions in atomic vapors.[2-4] In this paper we discuss three-wave mixing processes in molecules where resonant enhancement is achieved via Stark tuning of the molecular energy levels. This interaction and its subsequent experimental observation[10] suggest a new type of electrooptical effect, namely single sideband generation by applied microwave frequencies. A theoretical derivation and calculations of the interaction for a three-level system are presented here, specialized to the case of a particular molecule (NH_2D). The experimental observations are discussed in the following paper.[10]

II. THEORY

The application of a dc electric field to a gas introduces a preferred spatial direction thus destroying the inversion symmetry. The second order induced polarization amplitude can then be related to the product of the field (complex) amplitudes by

$$P_\alpha^{\omega_1=\omega_3-\omega_2} = d_{\alpha\beta\gamma}^{\omega_1=\omega_3-\omega_2} E_{3\beta} E_{2\gamma}^* \quad . \tag{1}$$

Choosing the direction of the dc field as z, the allowed $d_{\alpha\beta\gamma}$ are d_{zzz}, d_{zii} and d_{izi}, where i = x or y.

In searching for a candidate gas in which to observe the effect one should look for molecules: (1) with a strong permanent dipole moment or (2) molecules which in the presence of a dc field acquire a large dipole moment so that the presence of the dc field constitutes an appreciable perturbation.

A molecule meeting criterion (2) is NH_2D. The molecule has, among others, the three levels shown in Fig. 1, which can be Stark-tuned into simultaneous resonance with the P(20) line of the CO_2 laser[11-14] and microwave radiation near 4 GHz as shown. This should lead to a strong resonant mixing of the P(20) line (of frequency $\omega_3/2\pi$) and the microwave field at $\omega_2/2\pi$ = 4 GHz, giving rise to the difference frequency radiation at $\omega_1 = \omega_3 - \omega_2$ when the Stark field is near E_{dc} = 3570 V/cm. Levels 1 and 2 belong to the lowest vibrational state ($\nu_2 = 0$) and have molecular angular momentum quantum numbers J = 4 and |M| = 4. The subscripts 04 and 14 correspond to the standard asymmetric top designation.[15] The symbols a (asymmetric) and s (symmetric) refer to the parity of the inversion-split vibrational wave functions. The application of an electric field E^{dc} causes an admixture of the wave functions $|4_{04}a\rangle$ and $|4_{14}s\rangle$ which is due to a non-vanishing matrix element of the molecular dipole operator connecting the two states. This admixture, which will soon be shown to be responsible for the nonlinear mixing, disappears at zero dc field. The parameter Δ appearing in the expression for the wave functions corresponds to the energy splitting $E_2 - E_1$ between the two low lying states and is given by

$$\Delta = [4|\langle 4_{04}a|\mu_z|4_{14}s\rangle|^2(E^{dc})^2 + \delta^2]^{1/2} \tag{2}$$

while the admixture wave functions are

$$|1\rangle = \frac{1}{\sqrt{2}}[\sqrt{1+\delta/\Delta}\ |4_{04}a\rangle + \sqrt{1-\delta/\Delta}\ |4_{14}s\rangle],\quad |2\rangle = \frac{1}{\sqrt{2}}[\sqrt{1-\delta/\Delta}\ |4_{04}a\rangle - \sqrt{1+\frac{\delta}{\Delta}}\ |4_{14}s\rangle]$$

where δ is the zero field splitting and μ_z is the projection of the molecular dipole moment operator along the direction of the dc field.

The expression for the nonlinear dipole moment of an NH_2D molecule depends on matrix elements which can be determined from linear absorption data as well as from the data on Stark splitting. This makes possible, in principle, a precise theoretical derivation of the nonlinear mixing behavior of this molecule and of its parametric dependencies.

Applying second order perturbation theory[16] to the three-level system of Fig. 1 and keeping only resonant (i.e., with near vanishing denominator) term leads to the following expression for the polarization generated at $\omega_1 = \omega_3 - \omega_2$ by the applied fields at ω_2, ω_3:

$$P_\alpha^{(2)}(t) = \frac{1}{4\hbar^2}\left\{\frac{N_1(\bar{\mu}\cdot\bar{E}_3)_{13}(\bar{\mu}\cdot\bar{E}_2^*)_{21}(\mu_\alpha)_{32}}{[\Gamma_{13}+i(\omega_3-\omega_{31})][\Gamma_{32}+i(\omega_1-\omega_{32})]}\right.$$

$$\left. - \frac{(N_2-N_1)(\bar{\mu}\cdot\bar{E}_3)_{13}(\bar{\mu}\cdot\bar{E}_2^*)_{21}(\mu_\alpha)_{32}}{[\Gamma_{12}+i(\omega_2-\omega_{21})][\Gamma_{32}+i(\omega_1-\omega_{32})]}\right\} e^{i\omega_1 t} \tag{3}$$

$$+ \text{c.c.}$$

where N_i is the population density of level i with $E_2 = E_3 = 0$.
At thermal equilibrium $N_2 \simeq N_1$ and the main contribution to $P_\alpha^{(2)}$ is from the first term, the one proportional to N_1.

At zero dc field the matrix element $(\mu_\alpha)_{32}$ is zero. This is due to the fact that, as can be shown by group theoretic arguments, only the molecular dipole moment along the b of NH_2D axis (μ_b), may possess a non-vanishing matrix element $\langle 5_{05}^a|\mu_b|4_{14}^s\rangle$, but $\mu_b = 0$ due to the basal plane symmetry of NH_2D. It follows from (3) that for $E_{dc} = 0$ no frequency mixing takes place. When $E_{dc} \neq 0$ the ground state wave function $|4_{04}^a\rangle$ is admixed into level 2 as shown in Fig. 1. This results in a non-vanishing matrix element $(\mu_a)_{32}$ proportional to $\langle 5_{05}^a|\mu_a|4_{04}^a\rangle$.

For $\bar{E}_2 || \hat{z}$, $\alpha = x$, and $\bar{E}_3 || \hat{x}$ we find, using the admixed wave functions, that the triple matrix element product appearing in (3) is given by

$$(\mu_z)_{21}(\mu_x)_{13}(\mu_x)_{32} = -4\mu_c \langle 4_{04}^a|\mu_x|5_{05}^a\rangle {}^2E_{dc}M^2\left(\frac{\delta}{\Delta^2}\right) \tag{4}$$

The dependence of the triple matrix element product on the dc electric field is contained in the factor $E_{dc}\,\delta/\Delta^2$ with Δ the energy separation between levels 2 and 1, as given by (2). The nonlinear mixing is thus absent, i.e., $P_x^{(2)} = 0$, at zero field ($E_{dc} = 0$) and at very high fields ($\Delta \gg \delta$). From (1) and (3) and using the fact that at room temperature $N_2 \tilde{=} N_1$, we obtain

$$d_{\alpha\beta\gamma}^{\omega_1=\omega_3-\omega_2} = \frac{1}{2\hbar^2}\,\frac{N_1(\mu_\gamma)_{21}(\mu_\beta)_{13}(\mu_\alpha)_{32}}{[\Gamma_{13}+i(\omega_3-\omega_{31})][\Gamma_{32}+i(\omega_1-\omega_{32})]} \tag{5}$$

Expression (5) applies to stationary molecules with energy levels at E_1, E_2 and E_3. In a gas sample we need to account for the Doppler shift of the transition energies of individual molecules. This is done by averaging the nonlinear coefficient $d_{\alpha\beta\gamma}$ over the Maxwellian velocity distribution function with the result for operation at line center, that

$$d_{\alpha\beta\gamma}^{\omega_1=\omega_3-\omega_2} = \frac{-N_1(\mu_\gamma)_{21}(\mu_\beta)_{13}(\mu_\alpha)_{32}}{2\hbar^2}\,\sqrt{\pi/2}\,\frac{c}{\sigma\omega_{31}}\,\frac{\partial F(x)}{\partial \Gamma} \tag{6}$$

where $F(x) = e^{x^2}\,\mathrm{erfc}(x)$, $\omega_{31} \simeq \omega_{32} \gg \omega_{21}$, $\Gamma_{13} \simeq \Gamma_{32} \equiv \Gamma$, $\sigma = \sqrt{kT/M}$ is the rms molecular velocity and $x = c\Gamma/(\sqrt{2}\sigma\omega_{31})$ is the ratio of the homogeneous (spontaneous plus pressure) linewidth Γ to the Doppler linewidth $\sqrt{2}\sigma\omega_{31}/c$.

Although a numerical estimate of the nonlinear mixing coefficient based on (6) is possible, a safer procedure and one that serves as a check on the matrix elements needed to evaluate d_{xxz} (the largest coefficient in NH_2D) is to relate it to the linear absorption coefficient of x polarized field at $\omega_3 = \omega_{31}$. The latter can be shown to be given (in esu units) by

$$\gamma_{31} = \gamma_H \sqrt{\pi}\, x e^{x^2}\,\mathrm{erfc}(x) \tag{7}$$

where γ_H is the value of γ_{31} at high pressures ($c\Gamma \gg \sigma\omega_{31}$) and is given by

$$\gamma_H = \frac{4\pi|\mu_{13}|^2\,\omega_{31}}{\hbar c\Gamma}\,N_1$$

Combining (6) and (7) leads after some mathematical manipulation to

$$d_{xxz}^{\omega_1=\omega_3-\omega_2} = -\frac{c(\mu_z)_{12}}{8\pi\hbar\omega_{31}}\left(\frac{\mu_{23}}{\mu_{13}}\right)\sqrt{\frac{\pi}{2}}\,\frac{c\gamma_H}{\sigma\omega_{31}}\left[2x^2F(x) - \frac{2}{\sqrt{\pi}}\,x\right] \tag{8}$$

The various constants in (8) are evaluated as follows: The matrix element $(\mu_z)_{12}$ is a function of the admixture and according to the wave functions (2) is given by

$$(\mu_z)_{12} = \frac{\delta}{\Delta}\,\langle 4_{04}^{a}|\mu_z|4_{14}^{s}\rangle \tag{9}$$

We obtain the matrix element $\langle a|\mu_z|s\rangle$ from comparing the splitting $E_2 - E_1$, as given by (2) to the experimental tuning curve of $E_2 - E_1$ vs. E^{dc}(14). This yields $\langle a|\mu_z|s\rangle = 1.14 \times 10^{-18}$ esu. At resonance $E^{dc} = 3570$ V/cm and $\delta/\Delta = 0.174$. These data are used in (9) and result in

$$(\mu_z)_{12} = 0.174\langle a|\mu|s\rangle = 0.198 \times 10^{-18} \text{ esu}$$

The saturated absorption γ_H and pressure broadening coefficient are obtained from the data on Ref. (13) as

$$\gamma_H = .028 \text{ cm}^{-1}$$

$$\Gamma/P = 2\pi(20.1 \text{ MHz/Torr}).$$

With these data we obtain

$$d_{xxz}^{\omega_1=\omega_3-\omega_2} = 2.31 \times 10^{-7} G(x) \text{ esu} \tag{10}$$

$$G(x) = 2x\left[\frac{1}{\sqrt{\pi}} - x\, e^{x^2} \operatorname{erfc}(x)\right] \tag{11}$$

The theoretical dependence of d_{xxz} on pressure (Eq. 10) is plotted in Fig. 2. The peak occurs at $P = 2.0$ Torr and has a value of

$$\left(d_{xxz}^{\omega_1=\omega_3-\omega_2}\right)_{max} = 6.4 \times 10^{-8} \text{ esu} = 2.4 \times 10^{-22} \text{ MKS}$$

A comparison of this predicted behavior with experiment is given in the adjoining paper.

The coefficient d estimated above refers to the generation of sideband radiation at ω_1 by mixing a CO_2 P(20) line with a microwave field ω_2 (at 4.1 GHz). It is thus appropriate to compare it to the electro-optic coefficient r_{41} of GaAs which can be used, alternatively, to generate the sideband by conventional electrooptic modulation.

Using the correspondence[17]

$$r_{j\ell k} = - \frac{2\varepsilon_o}{\varepsilon_j \varepsilon_\ell} d_{jk\ell} \tag{12}$$

we have

$$\frac{(n^3 r)_{NH_2D}}{(n^3 r)_{GaAs}} \sim 0.8 \tag{13}$$

We thus reach the conclusion that for sideband generation, dc biased NH_2D at $P \simeq 2$ Torr is comparable to GaAs (which is one of the best infrared modulation materials). We must recognize, however, that this large coefficient was obtained by exploiting the resonant nature of the effect. The penalty we pay for this is that of reduced bandwidth.

III. CONCLUSIONS

In conclusion, we have shown in detail how Stark admixing can give rise to second order optical nonlinearities in gases. We have derived an expression for the coefficient describing the mixing of an infrared and a microwave field in NH_2D. Available absorption data was used to obtain a numerical estimate for the mixing and to describe its parametric dependence. An experimental demonstration of this effect is described in the following paper.[10]

REFERENCES

1. J. F. Ward and G. H. C. New, "Optical third harmonic generation in gases by a focused laser beam," Phys. Rev., vol. 185, pp. 57-72, Sept. 1969.

2. J. F. Young, G. C. Bjorklund, A. H. Kung, R. B. Miles, and S. E. Harris, "Third-harmonic generation in phase-matched Rb. vapor," Phys. Rev. Lett., vol. 27, pp. 1551-1553, Dec. 1971.

3. A. H. Kung, J. F. Young, G. C. Bjorklund, and S. E. Harris, "Generation of vacuum ultraviolet radiation in phase-matched Cd. vapor," Phys. Rev. Lett., vol. 29, pp. 985-988, Oct. 1972.

4. K. M. Leung, J. F. Ward, and B. J. Orr, "Two-photon resonant, optical third-harmonic generation in cesium vapor," Phys. Rev., vol. 9A, pp. 2440-2448, June 1974.

5. R. S. Finn and J. F. Ward, "dc-induced optical second-harmonic generation in the inert gases," Phys. Rev. Lett., vol. 26, pp. 285-289, Feb. 1971.

6. J. F. Ward and I. J. Bigio, "Molecular second- and third-order polarizabilities from measurements of second-harmonic generation in gases," Phys. Rev., vol. 11A, pp. 60-66, Jan. 1975.

7. S. E. Harris and D. M. Bloom, "Resonantly two-photon pumped frequency converter," Appl. Phys. Lett., vol. 24, pp. 229-230, Mar. 1974.

8. D. M. Bloom, J. Yardley, J. F. Young, and S. E. Harris, "Infrared up-conversion with resonantly two-photon pumped metal vapors," Appl. Phys. Lett., vol. 24, pp. 427-428, May 1974.

9. P. D. Sorokin, J. J. Wynne, and J. R. Lankard, "Tunable coherent IR source based upon four-wave parametric conversion in alkali metal vapors," Appl. Phys. Lett., vol. 22, pp. 342-344, Apr. 1973.

10. R. L. Abrams, C. K. Asawa, T. K. Plant, and A. E. Popa, "Stark induced three-wave mixing in molecular gases, II. Experiment," (following paper).

11. R. G. Brewer, M. J. Kelley, and A. Javan, "Precision infrared Stark spectra of $N^{14}H_2D$ using Lamb dip," Phys. Rev. Lett., vol. 23, pp. 559-563, Sept. 1969.

12. M. J. Kelley, R. E. Francke, and M. S. Feld, "Rotational-vibrational spectroscopy of NH_2D using high-resolution laser techniques, J. Chem. Phys., vol. 53, pp. 2979-2980, Oct. 1970.

13. T. K. Plant and R. L. Abrams, "Broadening and absorption coefficients in $N^{14}H_2D$," J. Appl. Phys., vol. 47, pp.4006-4008,Sept.1976. Earlier data on this absorption coefficient and pressure broadening rate was published by A. R. Johnston and R. D. S. Melville, Jr., "Stark-effect modulation of a CO_2 laser by NH_2D," Appl. Phys. Lett., vol. 19, pp. 503-506, Dec. 1971, but the more recent measurements are more accurate and substantially different.

14. T. A. Nussmeier and R. L. Abrams, "Stark cell stabilization of CO_2 laser," Appl. Phys. Lett., vol. 25, pp. 615-617, Nov. 1974.

15. C. H. Townes and A. L. Schawlow, Microwave Spectroscopy: New York: McGraw-Hill, 1955.

16. A. Yariv, Quantum Electronics, 2nd Ed. New York: J. Wiley and Sons, 1975, p. 556.

17. Ibid., Ch. 16.

FIGURE CAPTIONS

Fig. 1. Some of the energy levels relevant to the derivation of the nonlinear coefficient.

Fig. 2. Theoretical dependence of NH_2D nonlinear coefficient on pressure when the applied fields are exactly resonant with the Stark tuned energy levels.

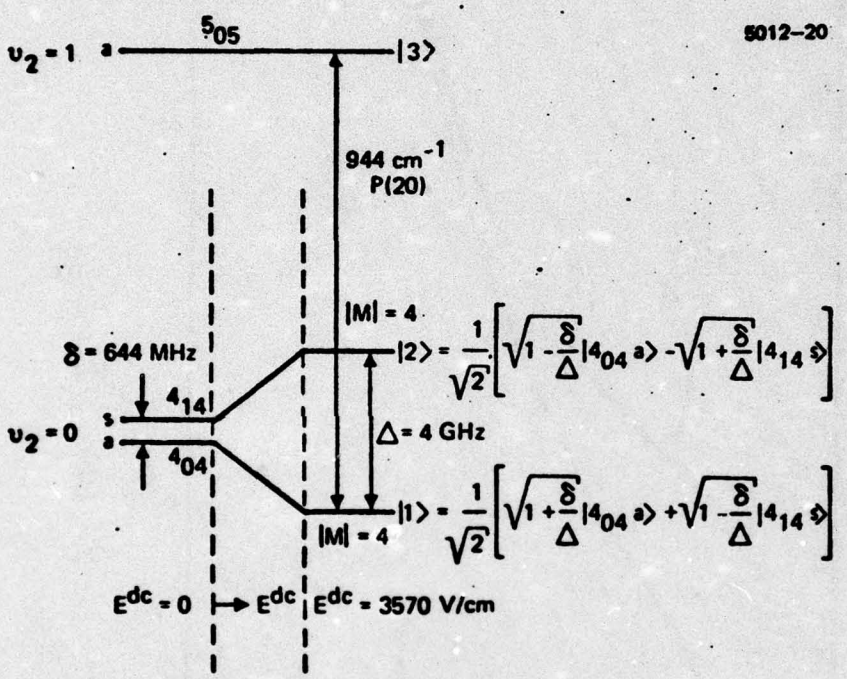

Fig. 1. Some of the energy levels relevant to the derivation of the nonlinear coefficient.

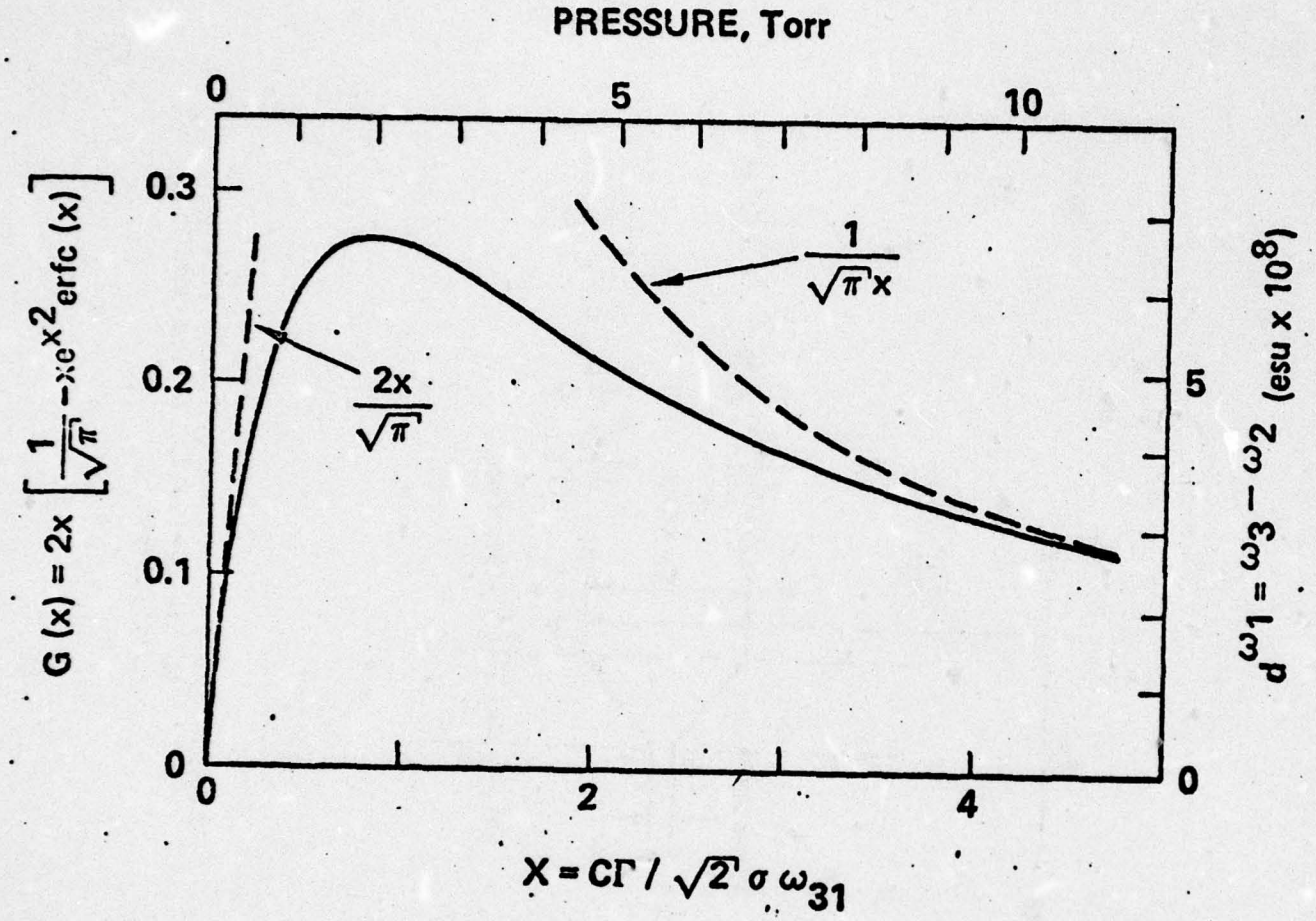

Fig. 2. Theoretical dependence of NH_2D nonlinear coefficient on pressure when the applied fields are exactly resonant with the Stark tuned energy levels.

APPENDIX B

Stark Induced Three-Wave Mixing in Molecular Gases*

II. Experiment

R. L. Abrams, C. K. Asawa, T. K. Plant, and A. E. Popa

Hughes Research Laboratories

Malibu, CA 90265

ABSTRACT

The first observation of resonantly enhanced, dc induced, three-wave mixing in a gas is presented. A cw CO_2 laser beam and microwave radiation at 4 GHz are mixed in a microwave Stark cell containing gaseous NH_2D. A single new sideband, 4 GHz below the applied CO_2 laser frequency, is observed with the aid of a scanning Fabry-Perot interferometer. The dependence of the sideband signal on gas pressure, microwave frequency, applied dc field, and microwave power are presented and compared with theoretical predictions.

* Research supported in part by the Advanced Research Projects Agency, monitored by the Office of Naval Research.

I. INTRODUCTION

In the accompanying paper,[1] it was predicted that a resonantly enhanced nonlinear mixing process in the molecule NH_2D could be induced by application of a dc electric field, where CO_2 laser radiation and microwave energy at 4 GHz interact producing a new single sideband 4 GHz below the applied laser frequency. We report here the first experimental observation of such single sideband optical modulation, unambiguously identified through the use of a scanning Fabry-Perot interferometer (SFP). We present measurements of the dependence of the parametric signal on gas pressure, microwave frequency, applied dc field, and microwave power. The results are all in good agreement with theoretical predictions although there is some uncertainty in the quantitative comparisons due to undetermined coupling losses in the microwave structure. Qualitatively, the agreement is excellent.

II. EXPERIMENTAL APPARATUS

The experimental apparatus for the observation of the interaction is discussed with reference to Fig. 1. A frequency stabilized cw CO_2 laser beam (operating at P(20) line center) is passed through the microwave Stark cell containing the Stark tunable gas. The cell consists of a 4 GHz ridged waveguide with an 8 mm wide ridge width, a 1.2 mm gap, 20 cm length, and forms a resonant cavity ($Q \sim 160$). The ridge is insulated from the rectangular structure by a thin layer of Mylar, allowing application of a dc Stark voltage and the 4 GHz microwave signal to the ridge. The microwaves are square wave modulated at 2 kHz, amplified in a TWT, and coupled into the ridged waveguide by means of a probe.

The output of the Stark cell is passed through a scanning Fabry-Perot interferometer (SFP) and detected with a HgCdTe photodiode. The SFP performs as a narrow bandwidth (300 MHz) optical filter that is slowly scanned through its 10 GHz free spectral range (FSR). The SFP output can then either be displayed directly on a recorder or synchronously detected at the microwave modulation frequency in a lock-in amplifier. Very small changes in the SFP output due to the presence of the microwaves were detectable with the latter method.

The NH_2D was prepared by introducing equal partial pressures of NH_3 and ND_3 in a mixing chamber. The resultant mixture containing 37.5% NH_2D was metered into the cell and the pressure monitored with a capacitance manometer.

III. RESULTS

Figure 2 shows the SFP output before and after lock-in detection with 1.1 Torr of gas in the cell. The two outputs are simultaneously displayed on a strip chart recorder as the SFP is scanned through one full order. The upper trace shows the direct SFP signal, with the familiar pattern of a single mode laser. This is the SFP spectrum of 10.6 μm carrier transmitted through the cell to the detector. The free spectral range (FSR) is 10 GHz (1.5 cm plate spacing). The lower trace of Fig. 2 shows the lock-in detection output with a 30 msec time constant. Signals occur at the positions corresponding to the peaks of the direct SFP output, indicating some sort of carrier modulation as a result of the applied microwave signal. A new peak, which is the parametric signal displaced

4 GHz from the carrier, appears approximately 40% of the way between the two carrier peaks. Note that only a single sideband occurs, for double sideband generation would result in two signal peaks lying between the two carrier signals. Calibration of the SFP has verified that the sideband is a lower one, as predicted, and corresponds to the difference frequency between the 10.6 μm carrier frequency and the microwave frequency. That the output is a parametric signal and not laser induced fluorescence from the gas is substantiated by the fact that the sideband is linearly polarized and no other line is observed in the SFP output; if the output were fluorescence, unpolarized emission at several wavelengths would be expected.

The parametric signal was measured as a function of the Stark voltage as shown in Fig. 3. The SFP sawtooth drive was disconnected and the mirror spacing was set to transmit the peak of the parametric sideband signal for these measurements. The maximum signal occurred at a Stark voltage of 428 V with the microwave frequency set at 4.023 GHz. The full width at half maximum (FWHM) of the signal was 28.5 V which is equivalent to a linewidth of $\sim$ 130 MHz. The linewidth of the signal is greater than the NH_2D linewidth at 1 Torr of 105 MHz[2] due to some inhomogeneities in the Stark gap. A measured low pressure absorption linewidth of 100 MHz FWHM compared to the 82 MHz actual doppler width indicates a 0.5% variation in the Stark gap spacing.

The Stark voltage was increased to 600 V and the $|M| = 3$ parametric signal was seen at $\sim$ 570 V. The ratio of the $|M| = 3$ to the $|M| = 4$ signal amplitudes was 0.414. A theoretical calculation of this intensity ratio yields a predicted signal ratio of .40. The agreement is well within experimental error.

The parametric signal was measured as a function of the Stark cell pressure over a range of 0 to 8 Torr as shown in Fig. 4. The SFP was set to transmit the maximum signal and the microwave frequency was fixed at 4.023 GHz. The parametric signal rose slowly between 0 and 0.5 Torr, then rose sharply between 0.5 and 1.5 Torr, reaching a maximum at 2.4 Torr. The signal slowly decreased between 3 and 8 Torr. The experimental curve and theory were compared using the best current NH_2D parameters with the theoretical points also shown on Fig. 3. Here the experimental "effective" Doppler width of 100 MHz was used to include the effects of the gap inhomogeneities. Again, the excellent agreement enforces the theory.

The parametric conversion efficiency varied linearly with microwave power, reaching 0.2% at the maximum available TWT output of 4 W. Microwave power saturation effects are anticipated when the microwave perturbation is comparable with the absorption linewidth ($\mu \cdot E_{RF} \sim 100$ MHz). This occurs at a field strength of $E_{RF} \sim 4 \times 10^4$ V/m. Unfortunately, unknown coupling losses prevent determination of the actual field strength. In the following paragraphs, we use theory, including the effects of phase mismatch and linear absorption, to calculate the theoretical conversion efficiency.

IV. COMPARISON WITH THEORY

The experiment involves traveling wave mixing between an input CO_2 laser (ω_3) and a microwave field at ω_2 ($\sim$ 4 GHz) to generate the difference frequency at $\omega_1 = \omega_2 - \omega_3$. The interaction is described by the following coupled mode equations,[3] which include the effects of optical losses and phase mismatch.

$$\frac{dA_1}{dx} = -\frac{\alpha_1}{2} A_1 - i \frac{g}{2} A_3 e^{-i\Delta kx}$$

$$\frac{dA_3}{dx} = -\frac{\alpha_3}{2} A_3 - i\frac{g}{2} A_1 e^{i\Delta kx} \qquad (1)$$

where

$$A_i(x) \equiv \sqrt{\frac{n_i}{\omega_i}}\, E_i(x)$$

$$g = \sqrt{\frac{\mu_0}{\varepsilon_0} \frac{\omega_1 \omega_3}{n_1 n_3}}\, d_{xxz}^{\omega_1 = \omega_3 - \omega_2} E_2$$

$$\Delta k = k_3 - (k_1 + k_2).$$

Assuming a single input $A_3(0)$ at $x = 0$, the solution of (1) yields a conversion efficiency η of

$$\eta(x) \equiv \left| \frac{A_1(x)}{A_3(0)} \right|^2 = \frac{g^2}{2\gamma} \exp\left(-\frac{\alpha_1+\alpha_3}{2} x\right) \left[\cosh\left(\sqrt{\gamma}\, x \sin(\theta/2)\right) - \cos\left(\sqrt{\gamma}\, x \cos(\theta/2)\right)\right] \qquad (2)$$

where

$$\gamma^2 = \left[\Delta k^2 + g^2 - \left(\frac{\alpha_1}{2} - \frac{\alpha_3}{2}\right)^2\right]^2 + \left[(\alpha_1 - \alpha_3)\Delta k\right]^2$$

$$\theta = \tan^{-1} \frac{(\alpha_1 - \alpha_3)\Delta k}{\Delta k^2 + g^2 - \left(\frac{\alpha_1}{2} - \frac{\alpha_3}{2}\right)^2}$$

The phase mismatch Δk occurs because both of the infrared signals travel through the cell colinearly and at the same velocity while the microwave wavefront travels in a guided mode. For our waveguide, we calculate that

$$\Delta k = 2\pi/\lambda_g - 2\pi/\lambda$$
$$= .08 \text{ cm}^{-1} \qquad (3)$$

where λ_g is the guide wavelength and λ is the free space wavelength.

The maximum possible conversion efficiency occurs at a pressure of 2.4 Torr. Assuming no microwave coupling losses, 4 W of input power and $Q \sim 160$ leads to $E_{RF} \sim 10^5$ V/m. At 2.4 Torr, $\alpha_3 = .02$ cm^{-1}, (see Ref. 2) $\alpha_1 = .014$ cm^{-1} and $g = .0138$ cm^{-1} giving a conversion efficiency in 20 cm of

$$\eta(20 \text{ cm}) = 1.1\% .$$

Due to asymmetric cavity coupling and a short $5\lambda_g/2$ cavity length, a large amount of the microwave energy is probably contained in higher order modes still present within the cavity. Assuming we only achieve 50% of the calculated microwave field in the lowest order mode, $E_{RF} = 5 \times 10^4$ V/m and an efficiency of .27% is expected in the 20 cm interaction length, a value close to that observed.

V. CONCLUSIONS

In conclusion we have observed a new type of electrooptic effect, namely single sideband infrared generation due to resonantly enhanced, dc induced, three-wave mixing in a gas. In the future we hope to increase the conversion efficiency to useful levels, although cw power levels suitable for local oscillator applications could be generated with the present device.

The authors wish to acknowledge the able technical assistance of R. E. Brower and R. R. Niedziejko in carrying out these experiments.

REFERENCES

1. R. L. Abrams, A. Yariv, and P. Yeh, "Stark induced three-wave mixing in molecular gases, I. Theory," (preceding paper).

2. T. K. Plant and R. L. Abrams, "Broadening and absorption coefficients in $N^{14}H_2D$," J. Appl. Phys., vol. 47, pp. 4006-4008, Sept. 1976.

3. A. Yariv, Quantum Electronics, 2nd Ed. New York: J. Wiley and Sons, 1975.

FIGURE CAPTIONS

Fig. 1. Experimental apparatus for observation of single sideband signal. The traveling wave tube amplifier (TWT) supplies up to 4 W to the Stark cell.

Fig. 2. Simultaneous signals observed.
(a) Directly from the detector.
(b) After phase sensitive detection as the SFP is scanned through one order. Note that the new feature due to the 4 GHz microwave signal appears as a single sideband 4 GHz away from the carrier.

Fig. 3. Variation of parametric sideband signal with Stark voltage, showing interaction with $|M| = 4$ and $|M| = 3$ lines.

Fig. 4. Parametric signal versus Stark cell pressure 0 to 8 Torr. The theoretical points are calculated for a pressure broadening coefficient of 40.2 MHz/Torr with an effective Doppler width of 100 MHz.

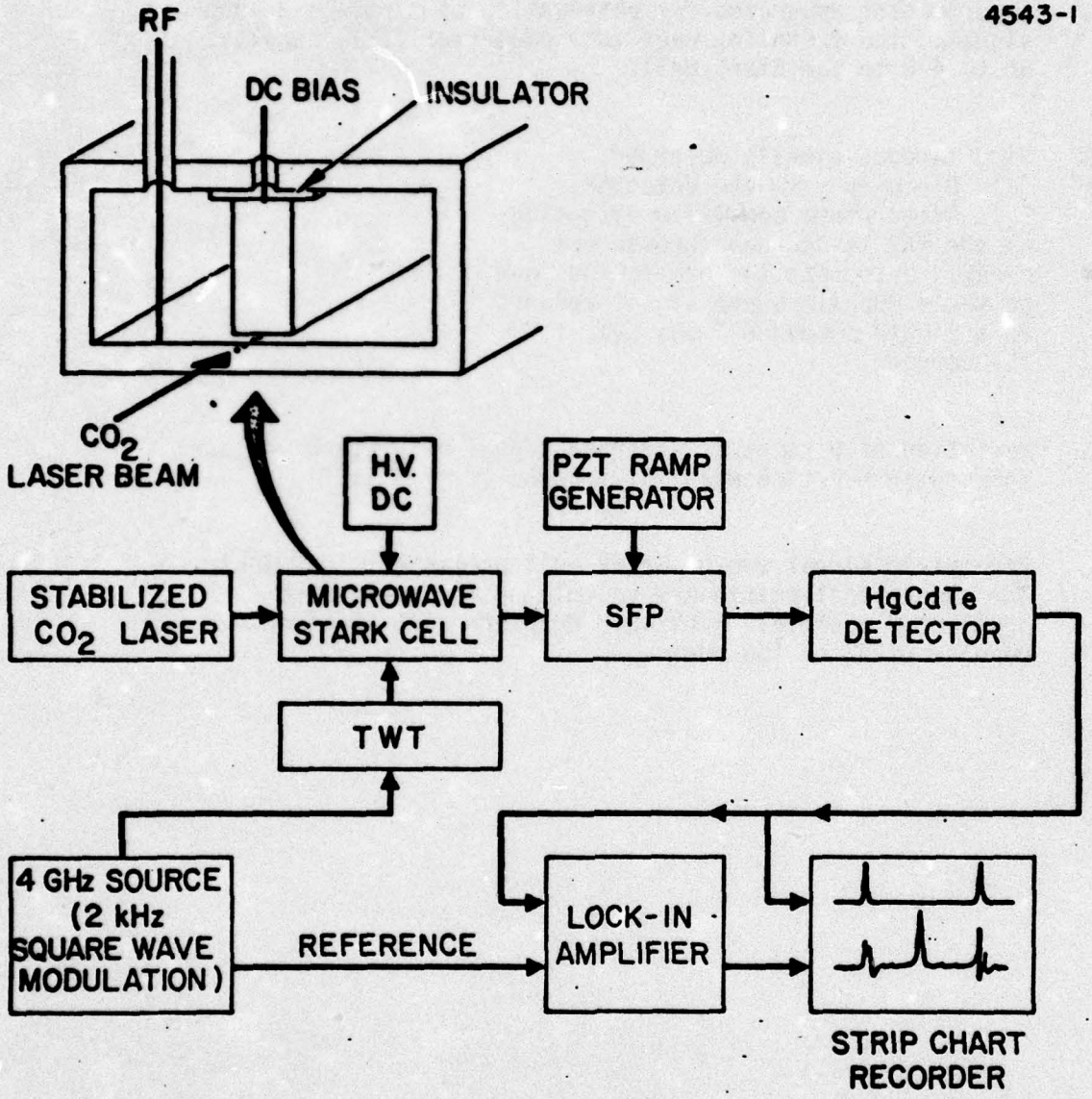

Fig. 1. Experimental apparatus for observation of single sideband signal. The traveling wave tube amplifier (TWT) supplies up to 4 W to the Stark cell.

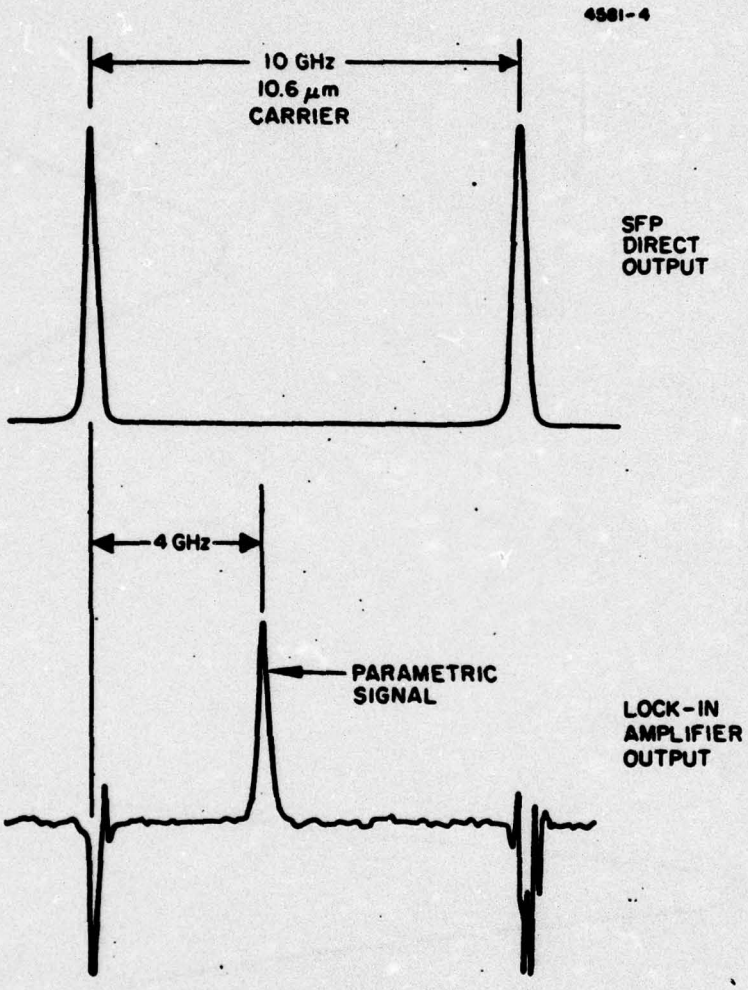

Fig. 2. Simultaneous signals observed.
(a) Directly from the detector.
(b) After phase sensitive detection as the SFP is scanned through one order. Note that the new feature due to the 4 GHz microwave signal appears as a single sideband 4 GHz away from the carrier.

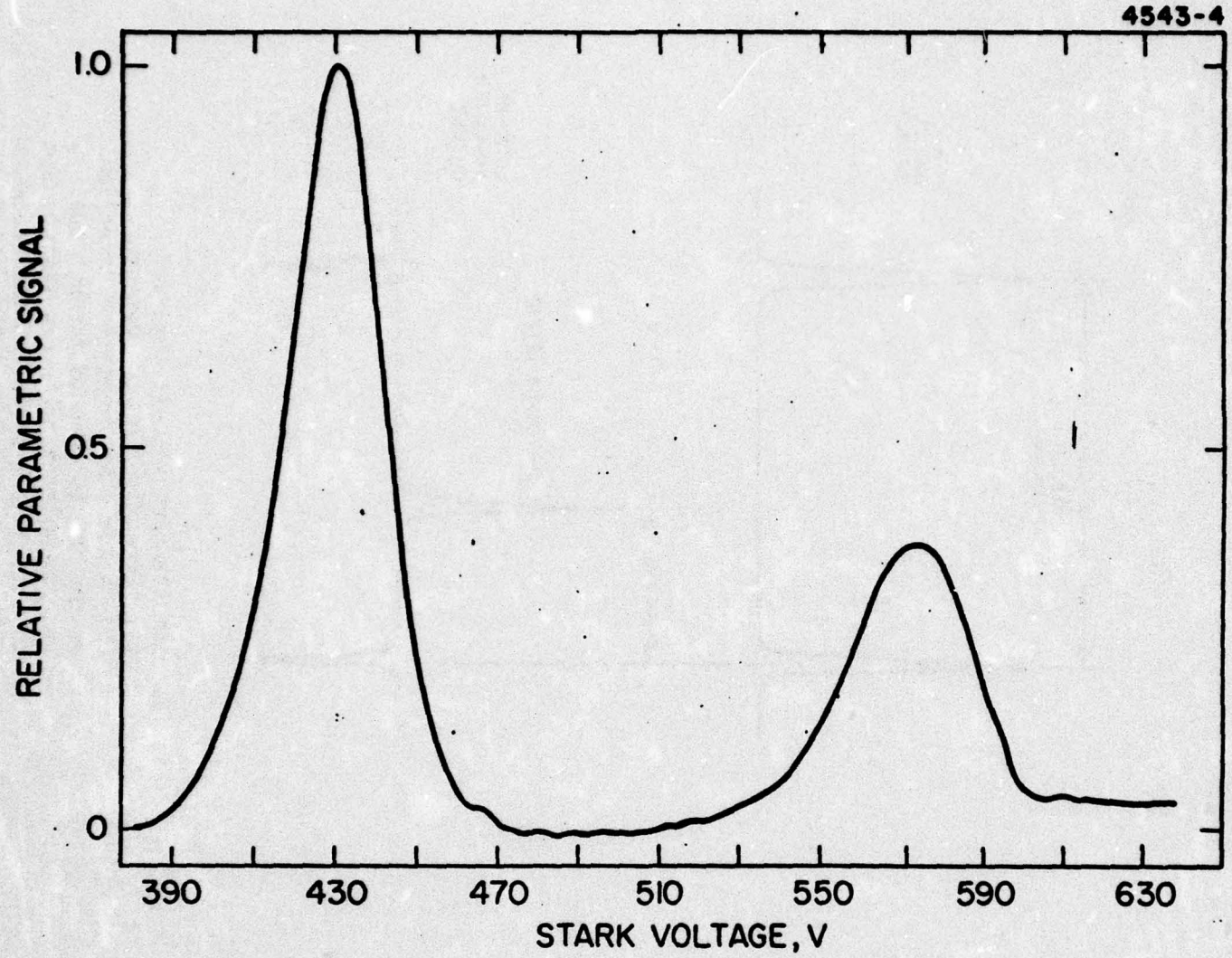

Fig. 3. Variation of parametric sideband signal with Stark voltages, showing interaction with |M| = 4 and |M| = 3 lines.

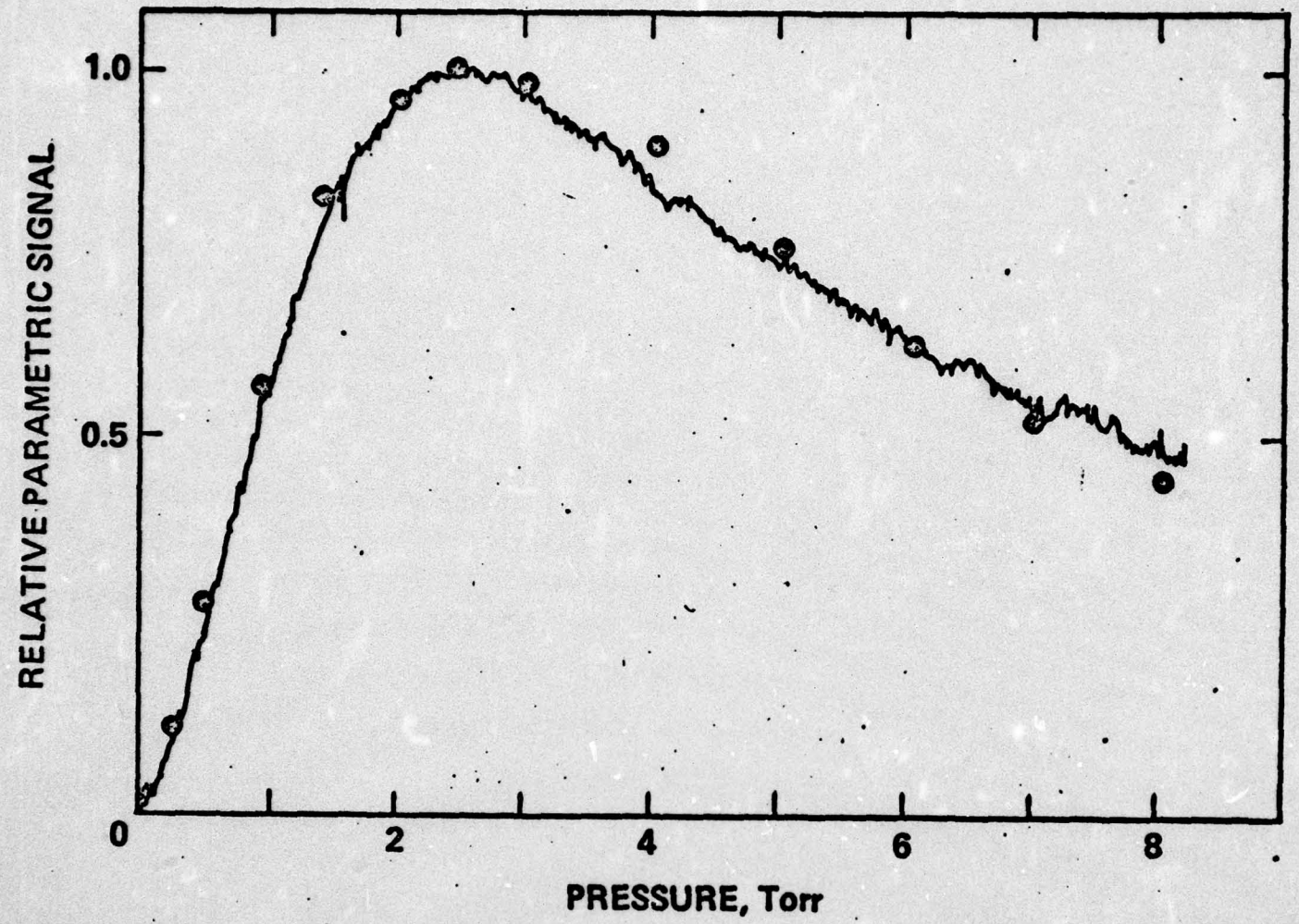

Fig. 4. Parametric signal versus Stark cell pressure 0 to 8 Torr. The theoretical points are calculated for a pressure broadening coefficient of 40.2 MHz/Torr with an effective Doppler width of 100 MHz.

APPENDIX C

Broadening and absorption coefficients in $N^{14}H_2D$

T. K. Plant and R. L. Abrams

Hughes Research Laboratories, Malibu, California 90265
(Received 12 April 1976)

The magnitudes of the pressure broadening and linear absorption coefficients have been measured for the Stark tunable $(0_a,4_{04},4)\rightarrow(1_a,5_{05},5)$ transition in $N^{14}H_2D$ using a CO_2 laser operating on the $P(20)$ 10.59-μm line. Two separate analysis methods give consistent results which are substantially different from values previously reported.

PACS numbers: 32.20.Pc, 42.30.Qw, 42.65.Dr, 42.60.Lh

The interaction of CO_2 laser radiation with Stark tunable absorption lines in molecules is proving to be of importance for CO_2 laser communications systems. Due to its unique energy level structure, $N^{14}H_2D$ has proven useful for laser modulation,[1] laser stabilization,[2] and, more recently, nonlinear optical interactions whereby a single sideband modulator operating at microwave frequencies was demonstrated.[3] For each of these applications it is necessary to know accurately both the magnitude and the linewidth of the absorption coefficient as a function of pressure. Johnston and Melville[1] reported values of 0.042 cm^{-1} for the high-pressure line-center absorption coefficient and 64 MHz/Torr full width half-maximum (FWHM) for the pressure-broadening coefficient. However, their Stark plate spacing showed a large nonuniformity evidenced by a measured low-pressure linewidth of 200 MHz FWHM in comparison with an expected Doppler width of 82 MHz.

In this paper we report new values for these parameters which were obtained by two separate methods. The absorption line shapes were fit to a Voigt profile from which the homogeneous linewidths were extracted. Second, the line-center absorption coefficients, corrected for overlapping $|M|=3$ absorption, were plotted as a log-log function of pressure from which the pressure-broadening coefficient was calculated. The agreement in the results from the two methods is excellent.

The experimental arrangement is shown in Fig. 1. The CO_2 waveguide laser source is Stark stabilized[2] at line center of the $P(20)$ 10.6-μm transition. One plate of the Stark absorption cell is grounded while the other plate is driven by a 9-Hz 300-V peak-to-peak square wave imposed on a slow sawtooth sweep varying from 240—350 V. Thus as the ramp voltage increases, the peak of the square wave is swept through the $|M|=4$ absorption of the $(0_a,4_{04},4)\rightarrow(1_a,5_{05},5)$ transition in $N^{14}H_2D$ whose center is at 450 V Stark voltage for our cell with a gap of 0.127 cm. The output of the Hg(Cd)Te detector is then phase sensitively detected at the 9-Hz square wave reference frequency. This low frequency is required due to the limited slewing rate of the high-voltage operational amplifier which must provide a very sharp voltage rise relative to the pulse width in order to avoid the gradual application of the resonant Stark voltage.

The total unabsorbed CO_2 signal level is found by chopping the laser beam with no applied Stark voltage and remains very stable during a run. Adequate attenuation is provided to avoid any power broadening in the gas or saturation of the detector. A slow sweep through the $N^{14}H_2D$ Stark resonance is made for gas pressures ranging from 50 μm to 10 Torr, yielding recorder plots of the corresponding absorption line shapes. By holding the laser frequency fixed and varying the Stark voltage to sweep through the absorption, problems of variation in laser intensity or detector sensitivity with frequency are avoided.

Since the $|M|=3$ absorption in $N^{14}H_2D$ lies only 150 V or ~670 MHz above the $|M|=4$ absorption, corrections must be made for the additional contribution of $|M|=3$ to the total absorption at higher pressures. This correction ranges from less than 1% at 4.5 Torr to ~7.5% at 10 Torr and was found from a series expansion of the total absorption given by

$$A_{\text{total}}=[1-\exp(-\gamma_4 l)]+[1-\exp(-\gamma_3 l)],$$

where γ_i is the absorption coefficient due to the $|M|=i$ transition and l is the length of the Stark absorption cell. In this case $l=10$ cm. The absorption coefficients are proportional to the line-shape function times a factor giving the relative intensities of the Stark components.[4]

The $N^{14}H_2D$ is formed by mixing two parts $N^{14}H_3$ and

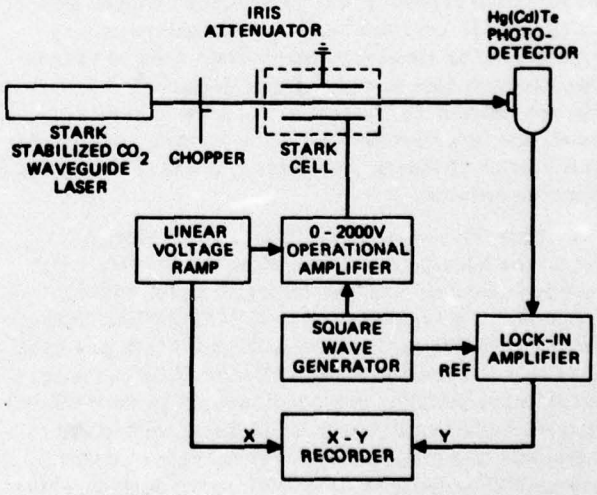

FIG. 1. Experimental arrangement for measuring absorption coefficient and linewidth of $N^{14}H_2D$ absorption.

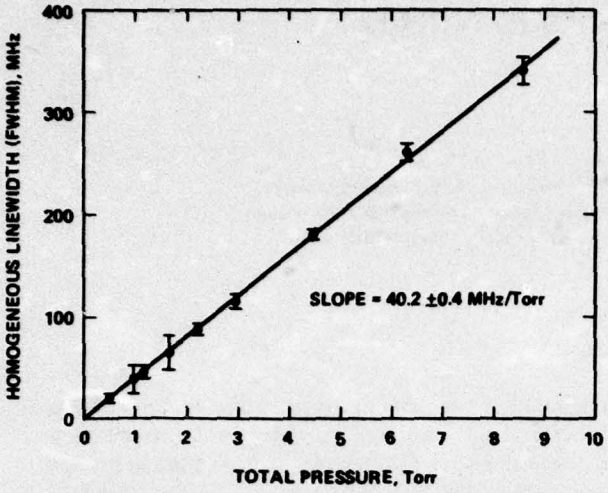

FIG. 2. Homogeneous linewidth extracted from Voigt profile fit to absorption line shapes versus Stark cell pressure. Effective $\Delta\nu_D = 84.5$ MHz (FWHM). Slope yields pressure-broadening coefficient.

one part $N^{14}D_3$ (98 at.% purity) and storing the resultant mix in a stainless-steel cylinder for future use. Evidence points to almost immediate mixing of these two species to yield a statistical mix of products of which ~45% is NH_2D. There is also evidence of changes in the gas composition, especially over the first few minutes in the Stark cell.

The cell consists of two pieces of precision-ground Al_2O_3, gold plated in the center electrode region, which are mated together and sealed in a stainless-steel can with small ZnSe AR-coated windows. Since NH_3 is known to adsorb to many surfaces, especially heavy metals, it is possible that any or all of the components are adsorbed to some extent thus changing the pressure in the cell. This was evidenced by a rapid decrease of up to 75% in the pressure of a clean cell filled with gas and sealed. If localized heating of the plates occurs from heating by the laser, there could even be breakdown products like N_2 or H_2 gases in the cell.[5] For the data presented here, however, care was taken to attenuate the laser and to allow time at each pressure for equilibration of the gas, so these processes should not affect the results.

In fitting the line-shape data to a Voigt profile to extract the homogeneous linewidths the Doppler width must be specified. The theoretical Doppler width for $N^{14}H_2D$ at room temperature is 82 MHz FWHM. However, a variation in the nominal 50-mil Stark gap spacing of only 0.18 mil is enough to add 5 MHz to the apparent Doppler width. Since our low-pressure (~50 μm) apparent Doppler width was 86±3 MHz, we decided to fit the data to a Voigt profile over a range of inhomogeneous widths from 82 to 89 MHz and pick those values from the best fit consistent with our measured value.

A computer program was available to fit the data to a Voigt profile.[6] Figure 2 shows the generated best homogeneous linewidths for various pressures and the best straight-line fit through zero to these values. The rms error in the fits is less than 3%, while the resulting linewidth error is less than 2%. The error bars are points at which the rms fitting error becomes twice its minimum value. The effective Doppler width giving the best straight line through zero is 84.5 MHz which agrees with our measured value within experimental error. The slope of the line is the pressure-broadening coefficient of 40.2±0.4 MHz/Torr.

A second determination of the pressure-broadening coefficient is made by examining the pressure dependence of the line-center absorption coefficient.[7] The line-center absorption coefficient in the high-pressure Lorentzian region is given by

$$\gamma(\lambda_0) = -\frac{1}{8\pi}\frac{\lambda_0^2}{\tau_{21}}\left(\frac{2}{\pi\Delta\nu_L}\right)\left(N_2 - \frac{g_2}{g_1}N_1\right),$$

where τ_{21} is the radiative lifetime of the transition, λ_0 is its wavelength, $\Delta\nu_L$ is the homogeneous linewidth (FWHM) and is proportional to pressure, and N_2 and N_1 are the populations of the upper and lower energy levels, respectively. Since N_2 and N_1 are also proportional to pressure, the pressure dependence cancels that of $\Delta\nu_L$, leaving $\gamma(\lambda_0)$ a constant.

In the low-pressure Doppler limit the line-center absorption coefficient is given by

$$\gamma(\lambda_0) = -\frac{1}{8\pi}\frac{\lambda_0^2}{\tau_{21}}\frac{2}{\Delta\nu_D}\left(\frac{\ln 2}{\pi}\right)^{1/2}\left(N_2 - \frac{g_2}{g_1}N_1\right),$$

where $\Delta\nu_D$ is the Doppler-broadened linewidth FWHM. Since $\Delta\nu_D$ is constant, $\gamma(\lambda_0)$ varies linearly with pressure as N_2 and N_1. Figure 3 is a log-log plot of $\gamma(\lambda_0)$ versus total cell pressure showing the linear behavior expected in both high- and low-pressure limits.

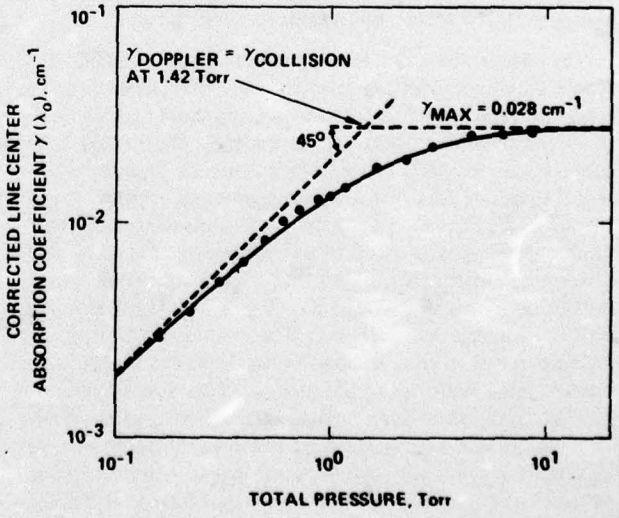

FIG. 3. Corrected line-center absorption coefficient ($|M| = 3$ effects subtracted) versus Stark cell pressure. Solid line is dependence predicted from Voigt profile using $\Delta\nu_D = 84.5$ MHz and $\Delta\nu_L = 40.3$ MHz/Torr.

The Voigt line shape leads to the following relation for the line-center absorption coefficient

$$\gamma(\lambda_0) = -\frac{1}{8\pi}\frac{\lambda_0^2}{\tau_{21}}\frac{a}{\Delta\nu_L(\pi)^{1/2}}\left(N_2 - \frac{g_2}{g_1}N_1\right)(1-\mathrm{erf}a) \times \exp(a^2),$$

where $a = (\Delta\nu_L/\Delta\nu_D)(\ln 2)^{1/2}$ and erf is the error function.[8] Using the values of $\Delta\nu_D = 84.5$ MHz and 40.3 MHz/Torr for the pressure-broadening coefficient in the above equation gives the curve shown in Fig. 3, which is an excellent fit to the experimental points.

The effective Doppler width (inhomogeneous linewidth) of 84.5 MHz is a combination of a theoretical 82-MHz Doppler width with ~2.5 MHz of broadening due to inhomogeneities in the Stark field of the absorption cell. Also shown in Fig. 3 is the predicted asymptotic behavior of the line-center absorption coefficient at both high and low pressures. The pressure-broadening coefficient is 40.2 ± 0.4 MHz/Torr and the high-pressure limit of the $|M| = 4$ transition line-center absorption coefficient is found to be $0.028\ \mathrm{cm}^{-1}$. Recent measurements of the transition dipole moment and collision rate using the Carr-Purcell echo technique are in excellent agreement with these values.[9]

In summary, we have used a fixed frequency source and a varying Stark field to trace out the $N^{14}H_2D$ absorption linewidths. From Voigt profile fits to the line shapes and from the line-center absorption coefficients, values of the pressure-broadening coefficient and the high-pressure absorption coefficient were found to be in good agreement. These more accurate values for this $N^{14}H_2D$ transition should prove valuable in the design of Stark cell devices for applications to problems in optical communications.

The authors are grateful for helpful discussions with C. K. Asawa and G. L. Tangonan and for the excellent technical assistance of R. E. Brower.

[1]A.R. Johnston and R.D.S. Melville, Jr., Appl. Phys. Lett. 19, 503 (1971).
[2]T.A. Nussmeier and R.L. Abrams, Appl. Phys. Lett. 25, 615 (1974).
[3]R.L. Abrams, C.K. Asawa, T.K. Plant, A.E. Popa, A. Yariv, and P. Yeh, 1976 International Quantum Electronics Conference, Amsterdam, The Netherlands, 1976, paper Q-5 (unpublished).
[4]C.H. Townes and A.L. Schawlow, *Microwave Spectroscopy* (McGraw-Hill, New York, 1955), p. 256.
[5]P.T. Dawson and R.S. Hansen, J. Chem. Phys. 48, 623 (1968).
[6]R.L. Abrams, Appl. Phys. Lett. 25, 609 (1974).
[7]E.T. Gerry and D.A. Leonard, Appl. Phys. Lett. 8, 227 (1966).
[8]T.K. McCubbin and T.R. Mooney, J. Quantum Spectrosc. Radiat. Transfer 8, 1225 (1968).
[9]R.L. Shoemaker and E.W. Van Stryland (private communication).

APPENDIX D

WIDEBAND MODULATION OF THE $C^{13}O_2^{16}$ LASER R(18) LINE AT 10.784 μm WITH AN $N^{14}H_3$ STARK CELL

C. K. Asawa and T. K. Plant

Hughes Research Laboratories
3011 Malibu Canyon Road
Malibu, California 90265

Intense Stark resonance absorptions near 10.7 μm of the R(18) and R(24) lines and a weaker absorption of the R(26) line of the isotopic $C^{13}O_2^{16}$ laser by $N^{14}H_3$ are reported. Wideband modulation experiments with an $N^{14}H_3$ Stark cell and the R(18) line are presented. Key modulation features are 2 nsec rise time, high modulation depths, low power dissipation, short Stark modulator cell (10 cm), high saturation intensity (>8 W/cm^2), new spectral features of the modulated signal versus Stark bias, and a demonstration of 180 Mbit random word modulation.

WIDEBAND MODULATION OF THE $C^{13}O_2^{16}$ LASER R(18) LINE AT 10.784 μm WITH AN $N^{14}H_3$ STARK CELL

Intense, low field Stark resonance absorptions of the R(18) and R(24) lines and a weaker absorption of the R(26) line of an isotopic $C^{13}O_2^{16}$ laser by $N^{14}H_3$ in a Stark cell have been observed and are described here. In addition, wideband Stark cell modulation experiments with the R(18) resonance are described. Key modulation features are 2 nsec rise time, high modulation depths, low power dissipation, short Stark modulator cell (10 cm), high saturation intensity (> 8 W/cm^2), new spectral features of the modulated signal versus Stark bias, and a demonstration of 180 Mbit random word modulation.

The near coincidence of the R-lines of the $C^{13}O_2^{16}$ laser and the transitions of $N^{14}H_3$ were examined by Allario and Seals[1] who pressure broadened the ammonia transitions at one atmosphere into coincidence with several R lines of the $C^{13}O_2^{16}$ laser. We examined the low pressure Stark resonance spectra of $N^{14}H_3$ with 25 of the more intense R and P lines in the 10 to 11 μm region of the isotopic $C^{13}O_2^{16}$ laser using Stark fields up to 20,000 V/cm. Intense Stark resonance absorptions were observed with the R(18) and R(24) lines, with a weaker absorption observed with the R(26) line. The R(18) line was determined to resonate with the asQ(6,6) transition of $N^{14}H_3$ and the R(24) line with the asQ(2,2) transition, the assignment being based on the laser frequencies reported by Freed et al[2] and the spectroscopic data of Shimizu.[3]

The R(18) absorption versus Stark voltage over a 0.153 cm Stark gap is shown in Fig. 1a. Absorption peaks occur at 1000, 1200, and 1500 V, corresponding to the $\Delta M = 0$ transitions ($E_{laser} \parallel E_{dc}$) between $|M| = 6,5$,

and 4 levels, respectively. The very high absorption of these transitions at low pressures is noted; nearly complete absorption of the $|M| = 6$ transition is attained at a pressure of 0.47 Torr and a path length of 10 cm. We measured the peak absorption coefficient for the $|M| = 6$ transition over a pressure range of 0.20 to 0.33 Torr on several different occasions. The measurements yielded an average peak absorption coefficient of 0.85 $\pm$ 0.15 cm^{-1} $Torr^{-1}$. Generally, lower values were obtained with older fills in the cell ($\gtrsim$15 min). This anomaly is unexplained, but may be associated with surface chemical interaction of the NH_3 and slight hydration of the ammonia. The laser power level entering the cell for these measurements was approximately 0.8 W/cm^2. We did not observe any evidence of power saturation of the absorption at levels up to 8 W/cm^2. The energy levels of $N^{14}H_3$ involved in the transitions are indicated in Fig. 1b.

The lowest Stark field resonance for the R(24) laser line appeared at a Stark voltage of 1800 V over a gap of 0.153 cm and is identified, using the results of References 2 and 3, as the asQ(2,2), $|M| = 2$, $\Delta M = 0$ transition. The resonance with the R(26) line occurring at 2400 V was not identified.

$C^{12}O_2^{16}$ laser modulation with a molecular Stark cell was initially described by Landman et al[4] and by several other investigators.[5-8] We examined the modulation characteristics of the $C^{13}O_2^{16}$ R(18)-$N^{14}H_3$ asQ(6,6) resonance, using a 10 cm length Stark cell with a gap of 0.153 cm and terminated with a 50 ohm load. The $N^{14}H_3$ gas pressure was between 0.45 and 0.55 Torr for the experiments described here. The modulated signal was

detected with a back-biased HgCdTe detector, the output being amplified with a wideband 1.2 GHz amplifier. Although the Stark field is biased in the quadratic Stark region, harmonic content of the modulated signal is down by 30 dB from the fundamental for a 10 V p-p sinusoidal modulation voltage.

Response of the Stark cell modulator to a sinusoidal signal and to a pseudo-random word generator was investigated. A typical steady state sinusoidal voltage response is shown in Fig. 2a. Application of a 40 V p-p sinusoid at 1 MHz resulted in a 44% depth of modulation. A bias voltage of 940 V was applied across the 0.153 cm gap. With increasing frequency the depth of modulation decreased (as shown later in Fig. 4).

The Stark modulator faithfully reproduced 180 MBit/s rate random words, as shown in Fig. 2b. A base-to-peak voltage of 7V applied to the Stark plates resulted in a 3.7% depth of modulation. The Stark bias voltage was 960 V over a 0.153 cm gap. The random word generator output was amplified by a flat 250 MHz bandwidth power amplifier, with the output being applied to the Stark plates terminated by a 50 ohm load. The upper frequency limit of the power amplifier somewhat deteriorated the random word applied to the Stark plate, as observed in Fig. 2b where the bits are triangular shaped. The modulator, however, responded faithfully to the deteriorated word. These experiments indicate that even higher bit rates with useful modulation depths should be attainable. A practical feature of this Stark modulator is that only a modest amount of power (<1 W) is required to attain useful modulation depths at high data rates.

The depth of modulation as a function of the amplitude of a 10 ns square wave applied to the Stark plates is shown in Fig. 3. Depth of modulation is defined as $(I_{max} - I_{min})/(I_{max} + I_{min})$ where I is the transmitted

laser intensity. The Stark bias was 960 V. The graph shows that the depth of modulation increases as the amplitude of the driving pulse is increased but saturates at higher voltages. Fig. 3b shows the oscilloscope traces of the modulator response to four different amplitudes of the Stark voltage square wave.

Finally, the power spectral response of the modulator to sinusoidal input for various Stark bias fields was examined. A sweep oscillator and amplifier (flat to $\pm$ 2 dB, 1 to 500 MHz) provided a 10 V pp sinusoid between 1 and 500 MHz to the Stark plates (0.153 cm gap). The modulated R(18) laser line was detected with a SAT HgCdTe photovoltaic detector whose response dropped by 3 dB at 300 MHz, by 8 dB at 400 MHz, and cut off at 460 MHz. The detected signal was fed to a spectrum analyzer.

Figure 4 shows the power spectral output for various Stark bias voltages (left side) and the Stark absorption spectrum for the $|M| = 5,6$, $\Delta M = 0$ transitions (right side). On the right side of Fig. 4 the various Stark bias voltages coincide with the positions of the R(18) laser line. For example, upon the application of 960 V Stark bias, the R(18) line coincides with position d on the Stark absorption spectrum. The relationship between the laser line position and the Stark bias in the Stark absorption spectrum can be seen more clearly with reference to the energy levels of Fig. 1a.

The spectral responses for various bias voltages, or equivalently various laser line positions, are shown on the left side of Fig. 4. As described above, a 10 V p-p sinusoid was added to the bias voltage, with the sinusoid frequency being swept from 1 to 500 MHz. Fluctuations in the spectral output at various frequencies due to impedance mismatches and

applied voltage variations have been smoothed out in Fig. 4, but the general character of the spectral response has been preserved. Typical fluctuations are shown as a dotted line for bias d.

Several features of the spectral response of Fig. 4 are noted. (1) Lower frequencies are attenuated with respect to the higher frequencies when the bias points or equivalently the laser line positions are at the tail of absorption curve, as at points a and b. This result suggests that the higher frequency response may be due mainly to the dispersive part of the resonance as suggested previously by Claspy and Pao.[5] (2) Harmonic contents were down by 30 dB from the fundamental (or below the noise level at 0 dB) for most bias voltages or laser positions except at points e, g, and i. At point e, the second harmonics at low frequencies were greater than the fundamental, as expected. (3) An unexpected dip in the response at 275 MHz occurred for the bias voltage of 1250 V (point j). The dip may arise from the interference between the absorptive part of the $|M| = 5$ transition and the dispersive part of the $M = 5$ and $M = 4$ transitions.

In summary, a potentially useful molecular Stark resonance of $N^{14}H_3$ with the R(18) line at 10.784 μm of the isotopic $C^{13}O_2^{16}$ laser has been described. Modulation experiments show that useful modulation at rates well above 180 Mbit/s appear to be attainable with this system.

We wish to acknowledge helpful discussions with R. L. Abrams, A. E. Popa and G. L. Tangonan and the expert technical assistance of R. E. Brower.

REFERENCES

1. F. Allario and R. K. Seals, Jr., Appl. Opt. 14, 2229 (1975).
2. C. Freed, A.H.M. Ross, and R. G. O'Donnell, J. Mol. Spectrosc. 49, 439 (1974).
3. F. Shimizu, J. Chem. Phys. 52, 3572 (1970).
4. A. Landman, H. Marantz and V. Early, Appl. Phys. Lett. 15, 357 (1969).
5. P. C. Claspy and Y. H. Pao, IEEE J. Quantum Electron. QE-7, 512 (1971).
6. A. R. Johnston and R.E.S. Melville, Appl. Phys. Lett. 19, 503 (1971).
7. J. M. Martin, V. J. Corcoran, and W. T. Smith, IEEE J. Quantum Electron. QE-10, 191 (1974).
8. M.M.T. Loy, Appl. Phys. Lett. 26, 99 (1975).

FIGURE CAPTIONS

Fig. 1 a) Low voltage Stark absorption spectrum of $N^{14}H_3$ with the isotopic $C^{13}O_2^{16}$ laser line R(18) at 10.784 μm. Pressure, 0.47 Torr; path length, 10 cm; Stark gap, 0.153 cm. Upper trace is the Stark voltage ramp. The "no transmitted light" trace was triggered separately.

b) Stark energy levels for the asQ(6,6) transitions, with $\Delta M = 0$, $|M| = 6, 5, 4$. Splitting of the excited state is assumed to be small.

Fig. 2 Modulated signal as a function of modulation applied to Stark cell.

a) 1 MHz sine, 40 p-p; 44% depth of modulation

b) 182 Mbit/s rate random word generator, 7 V p-p; 3.7% depth of modulation, Stark bias voltage 960 V.

Fig. 3 a) Depth of modulation for a 10 nsec pulse, as a function of applied pulse height. Stark bias voltage, 960 V. Depth of modulation is defined as $(I_{max} - I_{min})/(I_{max} + I_{min})$, where I is the transmitted laser intensity.

b) The sharp traces are the applied Stark voltages and the diffuse traces are the corresponding modulated output after detection.

Fig. 4 Modulated output spectrally analyzed as Stark cell was driven with a 10 V p-p sine wave swept from 1 to 500 MHz. Spectral response depended upon the Stark dc bias and therefore the position of laser line with respect to absorption line profile, as shown. The absorption spectrum versus Stark bias graph was taken at 0.50 Torr pressure. The abrupt drop in response at ~460 MHz was due to a detector-dewar resonance.

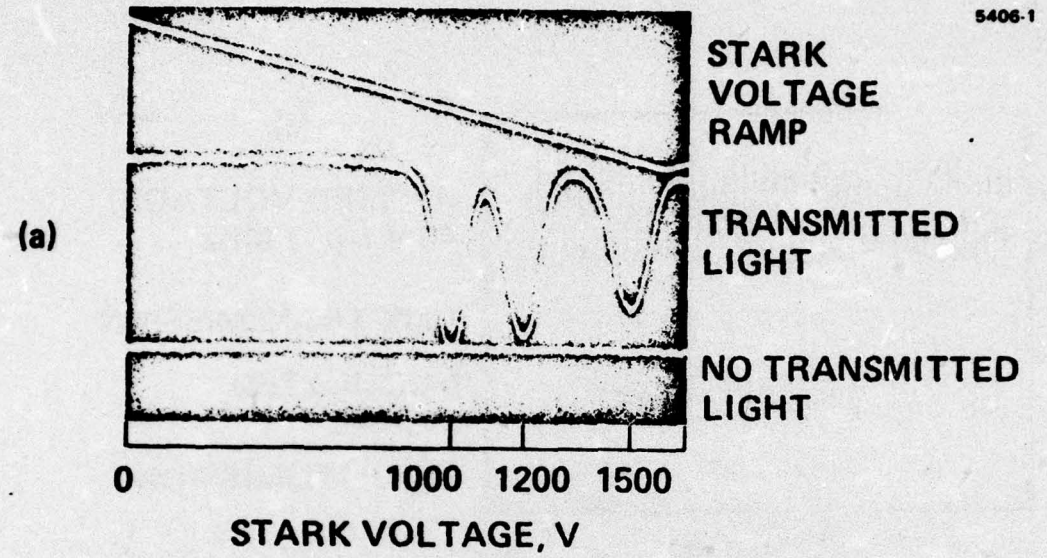
5406-1
(a)
STARK VOLTAGE RAMP
TRANSMITTED LIGHT
NO TRANSMITTED LIGHT
0
1000
1200
1500
STARK VOLTAGE, V

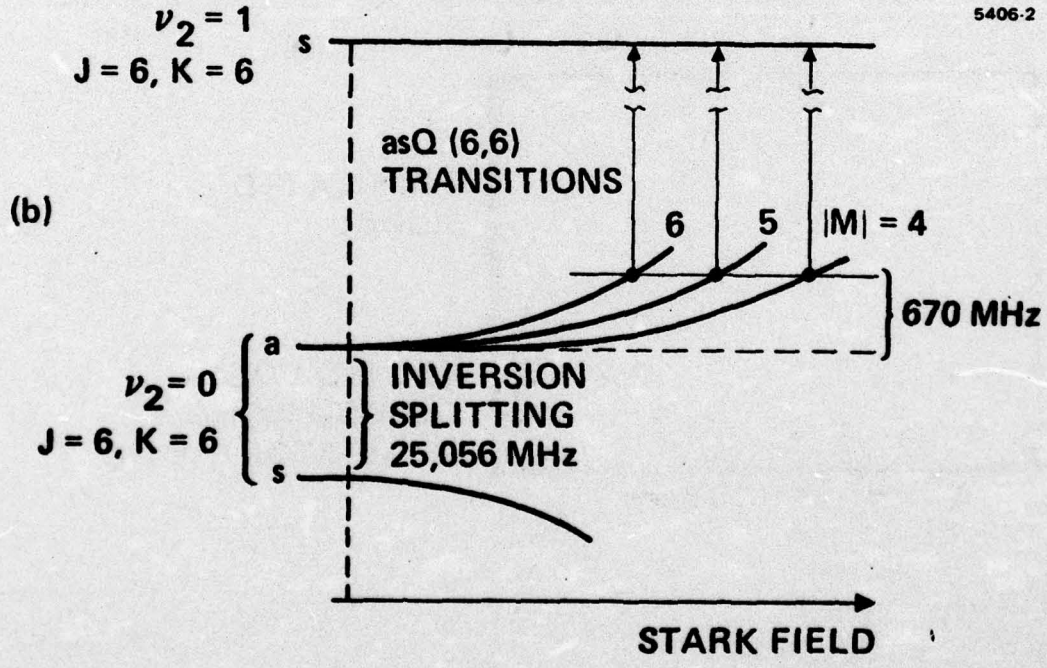
5406-2
(b)
$\nu_2 = 1$
J = 6, K = 6
s
asQ (6,6) TRANSITIONS
6
5
|M| = 4
670 MHz
a
$\nu_2 = 0$
J = 6, K = 6
INVERSION SPLITTING 25,056 MHz
s
STARK FIELD

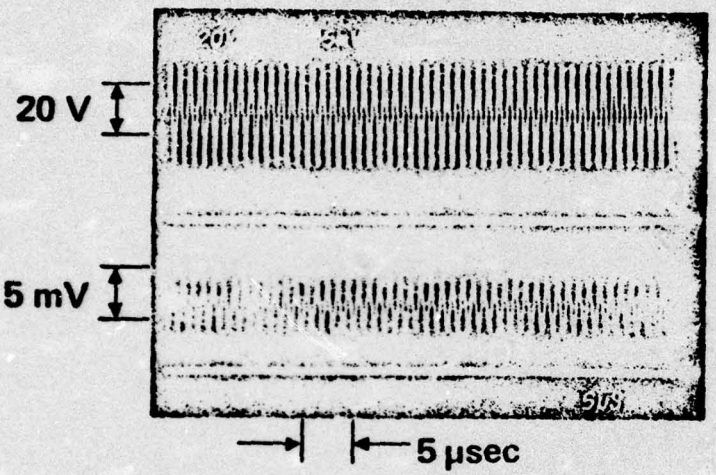

(a) 5406-3

APPLIED VOLTAGE, 40 V p-p, 1 MHz

100% TRANSMISSION

MODULATED SIGNAL

0% TRANSMISSION

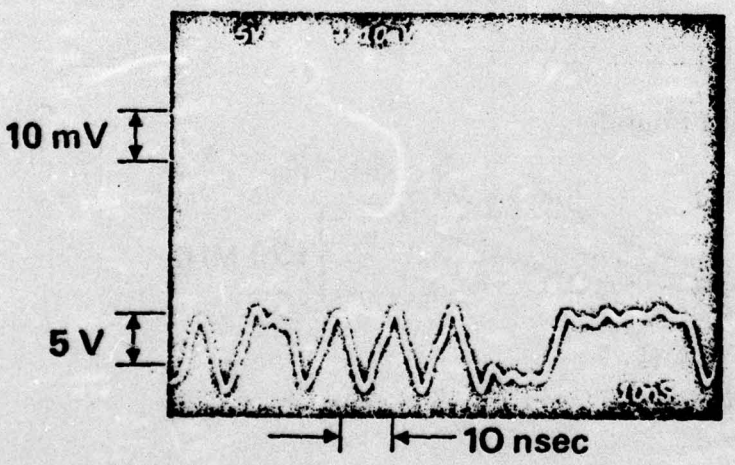

(b) 5406-4

MODULATED SIGNAL

APPLIED VOLTAGE, RANDOM WORD GENERATOR, 7 V p-p

5406-5

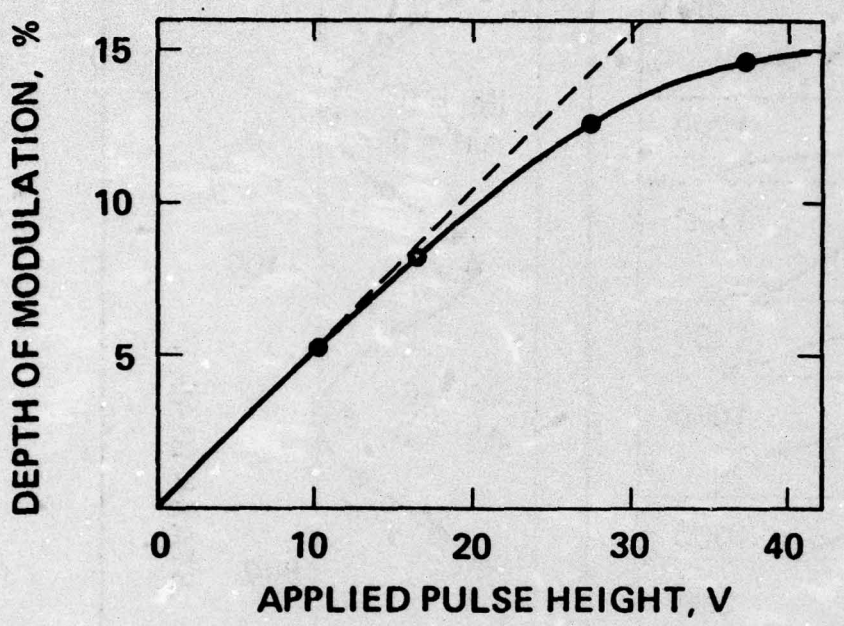
DEPTH OF MODULATION, %
15
10
5
0
10
20
30
40
APPLIED PULSE HEIGHT, V

(a)

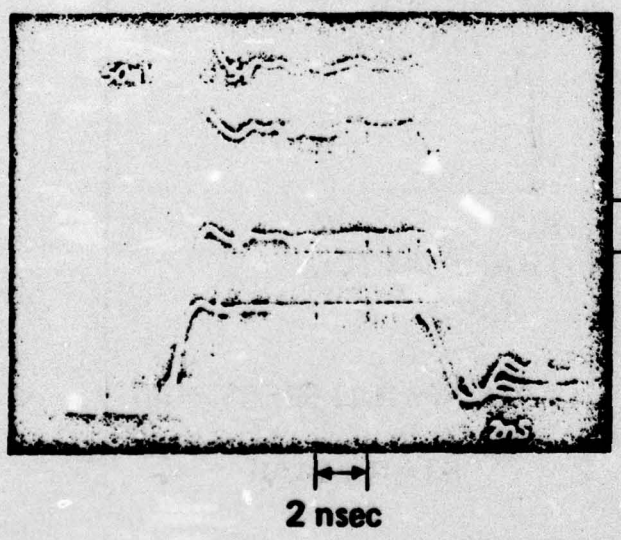
5V, APPLIED
50 mV, RESPONSE
2 nsec

(b)

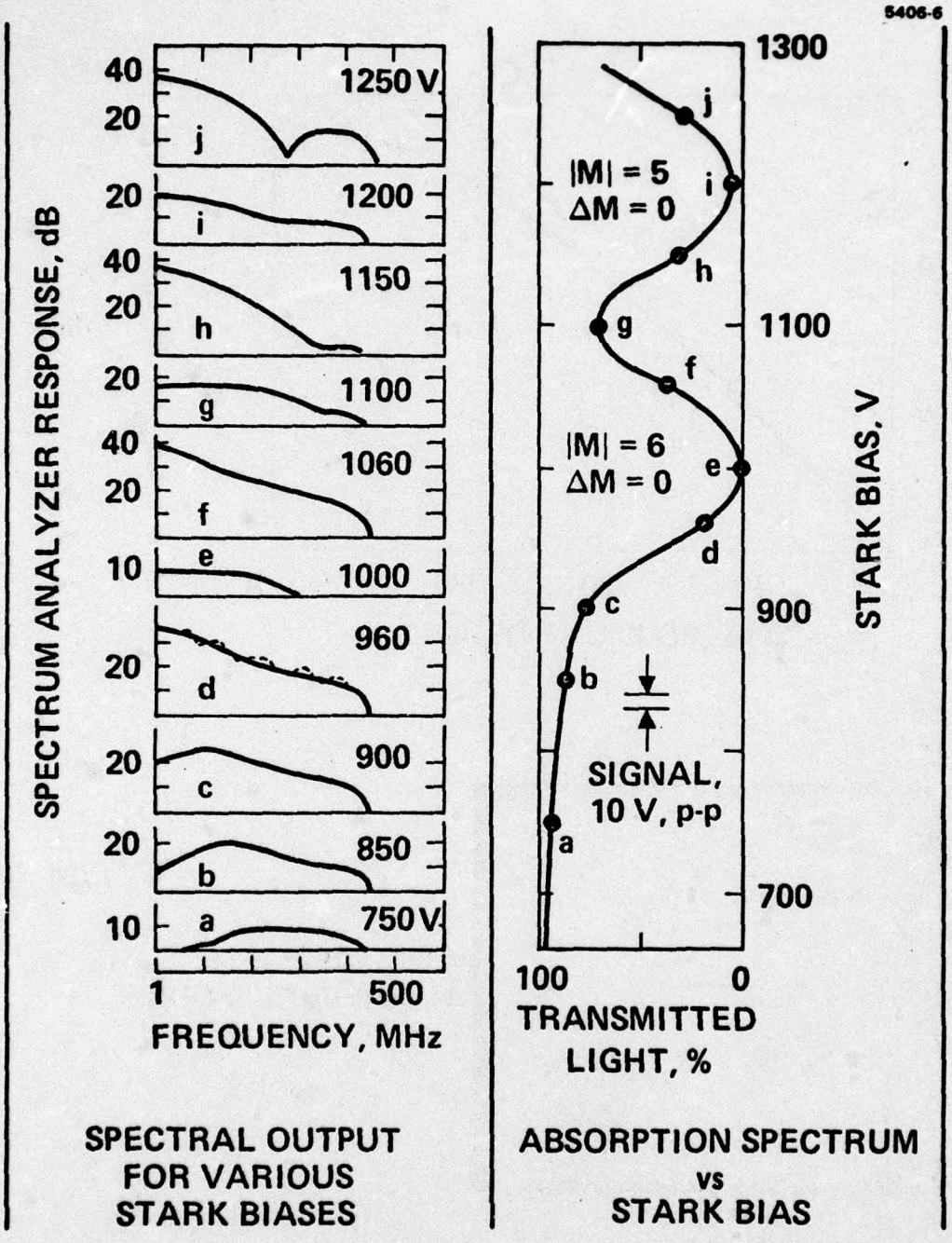

SPECTRAL OUTPUT FOR VARIOUS STARK BIASES

ABSORPTION SPECTRUM vs STARK BIAS